

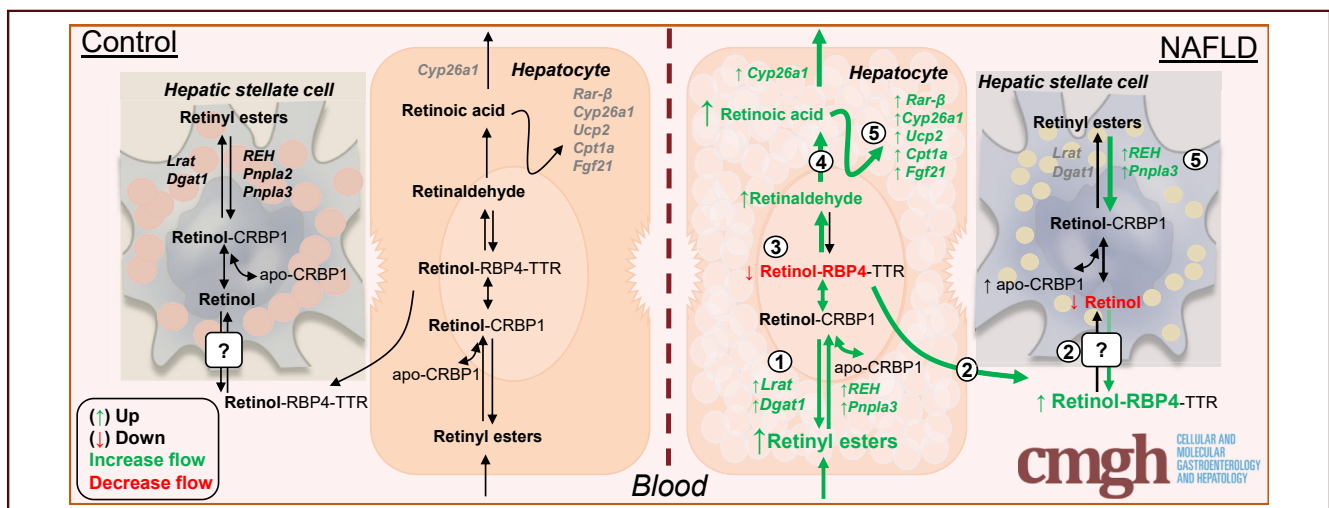
ORIGINAL RESEARCH

Impaired Hepatic Vitamin A Metabolism in NAFLD Mice Leading to Vitamin A Accumulation in Hepatocytes



Ali Saeed,^{1,2} Paulina Bartuzi,³ Janette Heegsma,^{1,4} Daphne Dekker,³ Niels Kloosterhuis,³ Alain de Bruin,^{3,5} Johan W. Jonker,⁶ Bart van de Sluis,³ and Klaas Nico Faber^{1,4}

¹Department of Gastroenterology and Hepatology, University Medical Center Groningen, University of Groningen, Groningen, the Netherlands; ²Institute of Molecular Biology and Biotechnology, Bahauddin Zakariya University, Multan, Pakistan; ³Section of Molecular Genetics, University Medical Center Groningen, University of Groningen, Groningen, the Netherlands; ⁴Laboratory Medicine, Department of Pediatrics, University Medical Center Groningen, University of Groningen, Groningen, the Netherlands; ⁵Dutch Molecular Pathology Center, Department of Pathobiology, Faculty of Veterinary Medicine, Utrecht University, Utrecht, the Netherlands; and ⁶Section of Molecular Metabolism and Nutrition, University Medical Center Groningen, University of Groningen, Groningen, the Netherlands



SUMMARY

Disturbed vitamin A metabolism in the liver of nonalcoholic fatty liver disease mice leads to cell type-specific redistribution of vitamin A, as a result of which hepatic retinol levels reduce but retinyl esters strongly accumulate in hepatocytes, rather than in hepatic stellate cells.

BACKGROUND & AIMS: Systemic retinol (vitamin A) homeostasis is controlled by the liver, involving close collaboration between hepatocytes and hepatic stellate cells (HSCs). Genetic variants in retinol metabolism (*PNPLA3* and *HSD17B13*) are associated with non-alcoholic fatty liver disease (NAFLD) and disease progression. Still, little mechanistic details are known about hepatic vitamin A metabolism in NAFLD, which may affect carbohydrate and lipid metabolism, inflammation, oxidative stress and the development of fibrosis and cancer, e.g. all risk factors of NAFLD.

METHODS: Here, we analyzed vitamin A metabolism in 2 mouse models of NAFLD; mice fed a high-fat, high-cholesterol (HFC) diet and *Leptin^{ob}* mutant (*ob/ob*) mice.

RESULTS: Hepatic retinol and retinol binding protein 4 (RBP4) levels were significantly reduced in both mouse

models of NAFLD. In contrast, hepatic retinyl palmitate levels (the vitamin A storage form) were significantly elevated in these mice. Transcriptome analysis revealed a hyperdynamic state of hepatic vitamin A metabolism, with enhanced retinol storage and metabolism (upregulated *Lrat*, *Dgat1*, *Pnpla3*, *Raldh3* and RAR/RXR-target genes) in fatty livers, in conjunction with induced hepatic inflammation (upregulated *Cd68*, *Tnfa*, *Nos2*, *Il1β*, *Il-6*) and fibrosis (upregulated *Col1a1*, *Acta2*, *Tgfβ*, *Timp1*). Autofluorescence analyses revealed prominent vitamin A accumulation in hepatocytes rather than HSC in HFC-fed mice. Palmitic acid exposure increased *Lrat* mRNA levels in primary rat hepatocytes and promoted retinyl palmitate accumulation when co-treated with retinol, which was not detected for similarly-treated primary rat HSCs.

CONCLUSION: NAFLD leads to cell type-specific rearrangements in retinol metabolism leading to vitamin A accumulation in hepatocytes. This may promote disease progression and/or affect therapeutic approaches targeting nuclear receptors. (*Cell Mol Gastroenterol Hepatol* 2021;11:309–325; <https://doi.org/10.1016/j.jcmgh.2020.07.006>)

Keywords: Fatty Liver Disease; Vitamin A; Autofluorescence.

See editorial on page 291.

Nonalcoholic fatty liver disease (NAFLD) is the most common liver disease worldwide. The prevalence of NAFLD is estimated at 20%–30% in the general population in Western countries. Starting with benign steatosis, patients are at risk to develop nonalcoholic steatohepatitis, and progress to cirrhosis and hepatocellular carcinoma.¹ NAFLD prevalence is particularly high in obese individuals (80%–90%), diabetes (30%–50%), or hyperlipidemia (90%).^{1,2} Hepatic fat accumulation is a combined result of a high fat- and high carbohydrate-containing diet and insufficient catabolism of these energy sources, in part owing to low physical activity.³ A tipping point NAFLD pathology is when simple steatosis is being accompanied by hepatic inflammation and fibrosis. Inflammation leads to the activation of hepatic stellate cells (HSCs) that transdifferentiate to proliferative and migratory myofibroblasts (eg, activated HSCs) that produce excessive amounts of extracellular matrix proteins, like collagens and fibronectins, the typical feature of fibrosis.⁴

HSCs are considered “quiescent” in the healthy liver, though they play a key role in controlling vitamin A metabolism.⁵ Vitamin A is important for many physiological processes, including reproduction, embryogenesis, glucose and lipid metabolism and vision, most of which are controlled by the retinoic acid-activated transcription factors retinoid X receptor (RXR) and retinoic acid receptor (RAR). Quiescent HSCs (qHSCs) contain the main body reserve of vitamin A, which is stored as retinyl esters in large cytoplasmic lipid droplets.^{6,7} Controlled conversion to retinol in qHSCs is believed to maintain stable circulating serum retinol levels around 2.0 $\mu\text{mol/L}$ in humans (1.0–1.5 $\mu\text{mol/L}$ in rodents). The specific (control) mechanisms involved are, however, largely unknown. Dietary vitamin A follows a complex route for final storage in HSCs.⁷ In the small intestine, retinyl esters are incorporated in chylomicrons and after transport through the circulation taken up by hepatocytes. In hepatocytes, they are converted to retinol and subsequent binding to retinol binding protein 4 (RBP4) stimulates the release of the retinol-RBP4 complex back to the circulation. Via an unknown mechanism, retinol is transferred to HSCs, re-esterified, and stored in lipid droplets. Liver injury-induced activation of HSCs leads to the rapid loss of vitamin A-containing lipid droplets and, as a consequence, chronic liver diseases are associated with vitamin A deficiency, including viral hepatitis, primary biliary cholangitis, primary sclerosing cholangitis, biliary atresia, alcoholic hepatitis, and also NAFLD.⁸ Vitamin A deficiency is defined as serum retinol levels below 0.7 mmol/L.⁹ Not only serum, but also hepatic retinol levels were found to be reduced in class III (body mass index $\geq 40 \text{ kg/m}^2$) obese patients and negatively correlate with histological severity of hepatic steatosis.^{10,11} These analyses, however, do not take retinyl esters into account, which form the largest pool of vitamin A. It thus remains unclear whether the low serum and hepatic retinol levels truly reflect complete depletion of vitamin A stores or, alternatively, point to aberrant vitamin A metabolism in the fatty liver. Notably, individuals carrying the NAFLD risk variant of *PNPLA3* (encoding adiponutrin) show low serum retinol levels, while hepatic retinyl ester levels are increased, pointing to impaired hepatic retinyl ester-to-retinol conversion.¹² The role of

disturbed vitamin A metabolism in the development of NAFLD has recently been further emphasized by the association of gene variants in *HSD17B13*, a retinol dehydrogenase, with hepatic steatosis.¹³ In addition, transcriptome analyses revealed a hyperdynamic state of hepatic retinol metabolism in NAFLD patients (eg, enhanced expression of genes involved in vitamin A storage, hydrolysis, and transport), though with unknown effects on the various vitamin A pools.¹⁴

Thus, in this study we analyzed serum and hepatic retinol, retinyl ester, and RBP4 levels in 2 NAFLD mouse models, as well as expression of genes and proteins involved in vitamin A metabolism. Our data show that NAFLD in mice does not lead to systemic vitamin A deficiency, but rather enhances vitamin A storage in the liver while retinol levels are reduced. Importantly, bulk of the vitamin A accumulates in hepatocytes, rather than in HSCs.

Results

High Fat, High Cholesterol Diet Increases Body Weight and Liver Fat Content

In order to study the effect of NAFLD on vitamin A metabolism, we fed mice a high fat, high cholesterol (HFC)-containing diet for 12 or 20 weeks and first confirmed the development of fatty liver disease. The HFC diet induced significant body and liver weight gain after 20 weeks (Figure 1A and B). Hepatic total and free cholesterol, as well as total triglycerides, were significantly increased after 12 weeks of HFC feeding and remained enhanced after 20 weeks (Figure 1C–E). Similarly, plasma total and free cholesterol, as well as insulin levels were significantly elevated HFC-fed mice (Figure 1F–H), hematoxylin and eosin and Oil Red O staining confirmed excessive fat accumulation in the livers of HFC-fed mice and was associated with accumulation of CD68-positive inflammatory cells (Figure 1I).


HFC Diet Induces Markers of Hepatic Lipid Uptake and Synthesis, Inflammation, and Fibrosis in Mice

Hepatic expression of genes involved in lipid uptake (*Srb1*, *Cd36*) and synthesis (*Scd1*, *Fasn*, *Acc1*, *Srebp1c*) were strongly induced in HFC-fed mice (Figure 2A). Moreover, the HFC diet leads to an early progression to steatohepatitis, with enhanced expression of inflammatory markers, including *Cd68*, *Tnf- α* , *Nos2*, *Ccl2*, *Il-1 β* , and *Il-6* (Figure 2B) as well as the progressive induction of markers of fibrosis (*Coll1a1*, *Acta2*, *Tgf- β* , and *Timp1*) (Figure 2C).

Reduced Retinol But Elevated Retinyl Palmitate in Livers of HFC-Fed Mice

Next, we determined the effect of the HFC diet on the levels of retinol in liver and plasma, as well as hepatic retinyl

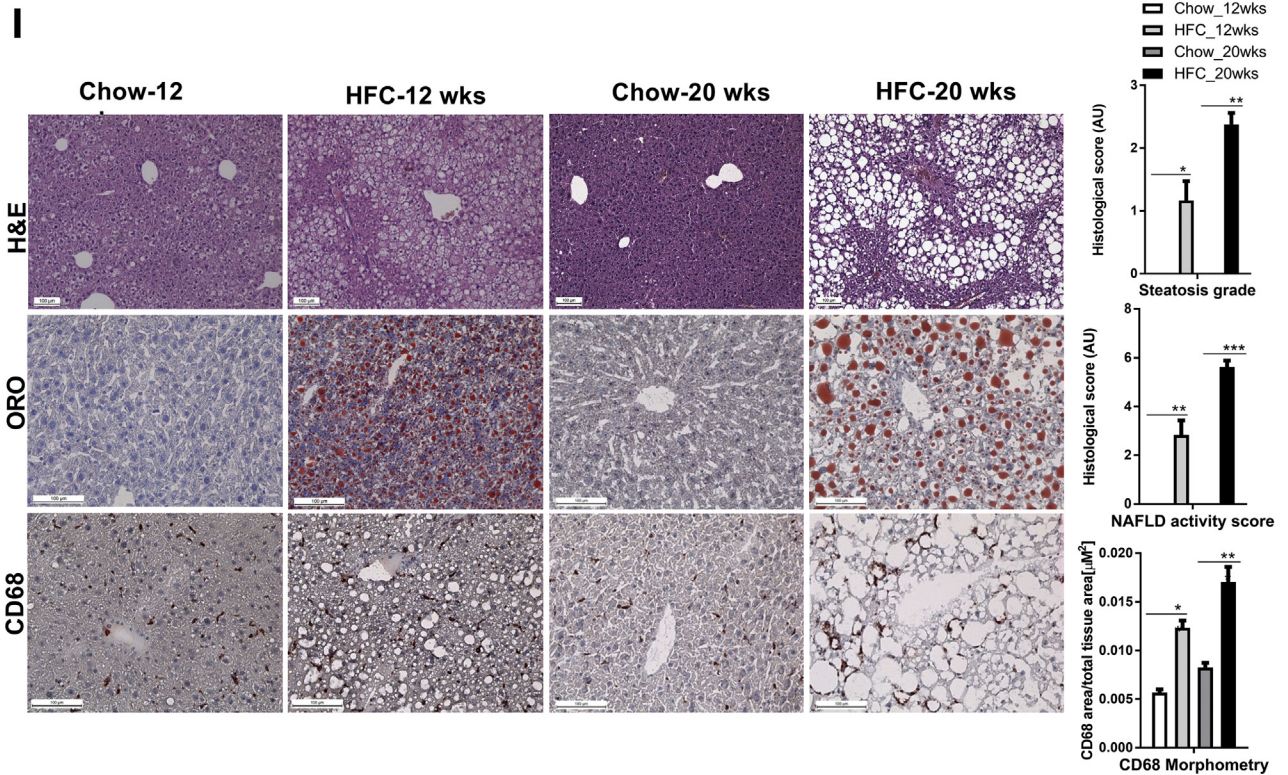
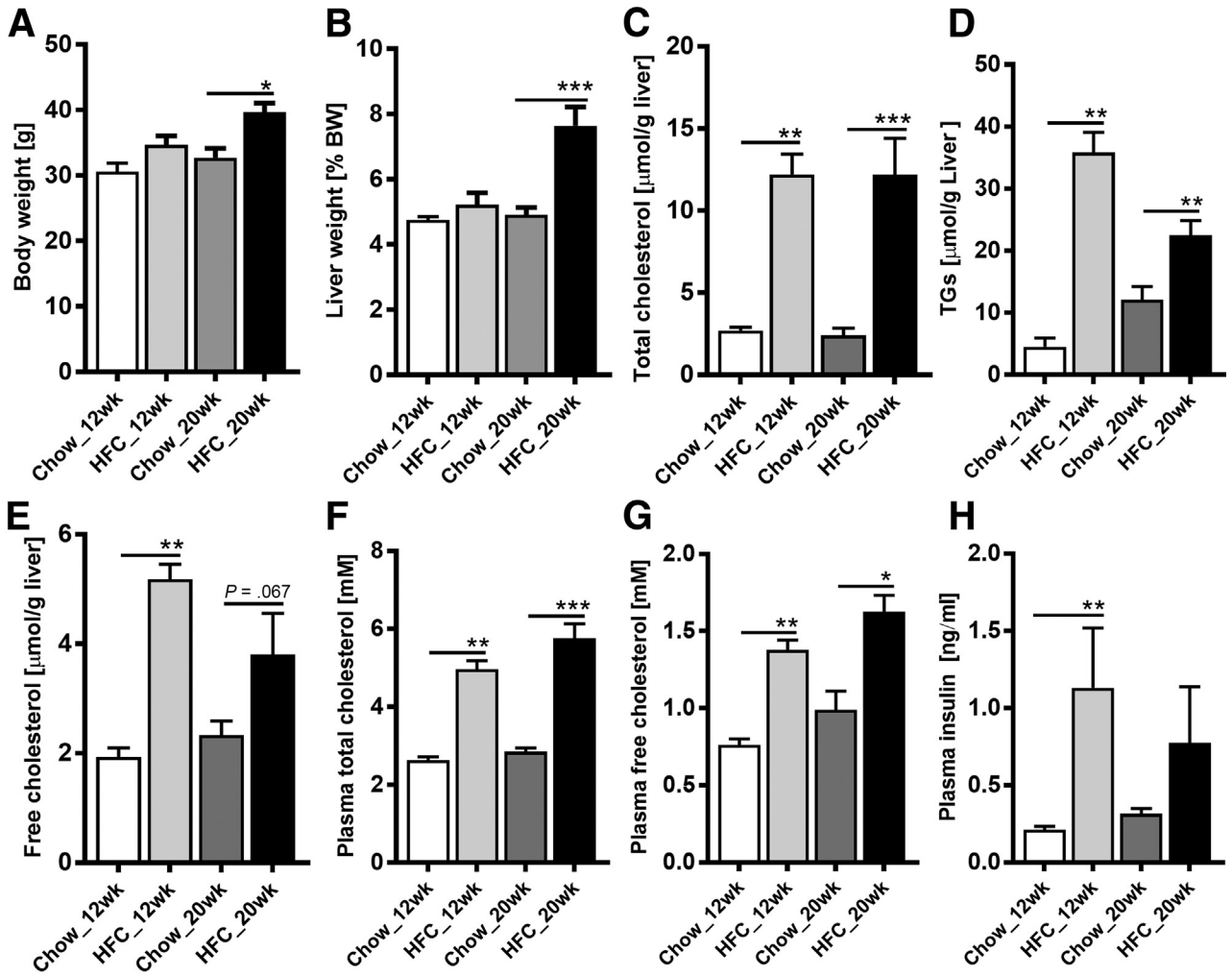
Abbreviations used in this paper: HFC, high-fat, high-cholesterol; HFD, high-fat diet; HSC, hepatic stellate cell; mRNA, messenger RNA; NAFLD, nonalcoholic fatty liver disease; qHSC, quiescent hepatic stellate cell; RAR, retinoic acid receptor; RBP4, retinol binding protein 4; RXR, retinoid X receptor.

 Most current article

© 2021 The Authors. Published by Elsevier Inc. on behalf of the AGA Institute. This is an open access article under the CC BY-NC-ND license (<http://creativecommons.org/licenses/by-nc-nd/4.0/>).

2352-345X

<https://doi.org/10.1016/j.jcmgh.2020.07.006>



palmitate, the major storage form of vitamin A. On the one hand, hepatic retinol levels were comparable in 12- and 20-week chow-fed mice (24.0 ± 2.4 and 24.0 ± 2.5 $\mu\text{g/g}$ liver, respectively) (Figure 3A). In contrast, hepatic retinol levels were progressively decreased in HFC-fed mice (9.1 ± 0.8 and 5.7 ± 0.8 $\mu\text{g/g}$ liver after 12 and 20 weeks, respectively) (Figure 3A). On the other hand, hepatic retinyl palmitate levels progressively increased in HFC-fed mice (785 ± 34 and $1,060 \pm 182$ $\mu\text{g/g}$ liver after 12 and 20 weeks, respectively) and were significantly higher than in chow-fed mice (331 ± 50 and 413 ± 58 $\mu\text{g/g}$ liver after 12 and 20 weeks, respectively) (Figure 3B). The disturbed hepatic retinol/retinyl palmitate balance was not accompanied by changes in plasma levels of retinol after a 12-week HFC diet (1.4 ± 0.1 and 1.6 ± 0.1 $\mu\text{mol/L}$ for chow and HFC diet, respectively), while it was increased in HFC-fed mice after 20 weeks (1.1 ± 0.1 and 2.1 ± 0.1 $\mu\text{mol/L}$ for chow and HFC diet, respectively) (Figure 3C). Hepatic RBP4 protein levels were decreased in HFC-fed mice compared with chow-fed mice (Figure 3D), while hepatic messenger RNA (mRNA) expression of *Rbp4* was comparable in all animal groups (Figure 4A). In contrast, serum RBP4 levels were elevated in HFC-fed mice, which was particularly evident after 20 weeks (Figure 3E). These results show that a drastic reduction in hepatic retinol levels in HFC-fed mice is accompanied by a significant increase in hepatic retinyl esters. Further, Pearson correlation analysis of tissue retinol levels showed a significant inverse correlation with tissue retinyl palmitate and plasma retinol levels, while tissue retinyl palmitate was not significantly correlated with plasma retinol (Figure 3F). Moreover, hepatic retinol levels in particular correlated inversely with biochemical and gene expression markers of NAFLD progression, including hepatic cholesterol and triglyceride levels, and hepatic expression of inflammatory (*Tnfa*, *Nos2*, *Ccl2*, and *Il1b*) and fibrosis (*Col1a1*, *Acta2*, *Tgfb*, and *Timp1*) markers (Supplementary Table 1).

Hepatic Expression of Genes Involved in Vitamin A Storage, Transport, and Hydrolysis as Well as Retinoic Acid Targets Are Elevated in HFC-Fed Mice

Hepatic mRNA levels of *Lrat*, coding for the main enzyme producing retinyl esters in the liver, increased with time in HFC-fed mice (Figure 4A). No or minor changes were detected in mRNA levels for alternative retinol-esterifying enzymes, like *Dgat1* and *Dgat2*. Of the various retinyl ester hydrolases that mobilize retinol from hepatic retinyl ester stores, only *Adpn/Pnpla3* mRNA levels were strongly induced in HFC-fed mice, while *Atgl/Pnpla2* and *Hsl/Lipe* mRNA levels were not altered compared with chow-fed mice. *Raldh2* mRNA levels were significantly enhanced in livers of HFC-fed mice, while levels of other members of the retinol to retinoic acid-converting enzymes¹⁵⁻¹⁷ were not changed (*Raldh1*, *Raldh3*, and *Raldh4*) (Figure 4B). Hepatic

expression of retinoic acid-responsive genes (*RAR- β* , *Cyp26a1*, *Hsd17b13*, *Ucp2*, *Cpt1a*, *Fgf21*) was enhanced in the mice fed the HFC diet (Figure 4C). Thus, an HFC diet leads to a hyperdynamic state of retinol metabolism in mice, confirming earlier observations in NAFLD patients.¹⁴

Reduced Retinol and Enhanced Retinyl Palmitate in Livers of *ob/ob* Mice

To validate our findings, we next analyzed hepatic vitamin A metabolism in another model of fatty liver disease (eg, the leptin-deficient *ob/ob* mouse). In line with the observations described previously for HFC-fed mice, hepatic retinol levels were significantly lower in *ob/ob* mice compared with age-matched wild-type littermates (2.8 ± 0.1 vs 16.9 ± 5.1 $\mu\text{g/g}$ liver, respectively) (Figure 5A), in conjunction with strongly enhanced levels of retinyl palmitate (359 ± 28 vs 160 ± 26 $\mu\text{g/g}$ liver, respectively) (Figure 5B). Moreover, plasma retinol and RBP4 levels were significantly higher in *ob/ob* mice as compared with their wild-type littermates (2.5 ± 0.2 vs 0.9 ± 0.2 μM retinol, respectively; (Figure 5C). Finally, also hepatic RBP4 protein levels were reduced in *ob/ob* mice independently of (unchanged) *Rbp4* mRNA levels as compared with wild-type mice (Figure 5D and 6A), all features being comparable between HFC-fed wild type mice and chow-fed *ob/ob* mice. Similar to HFC, plasma RBP4 levels were elevated in *ob/ob* mice as compared with wild-type mice (Figure 5E). Pearson correlation analysis of tissue retinol levels showed similarly a significant inverse correlation with tissue retinyl palmitate and plasma retinol levels, while tissue retinyl palmitate was not significantly correlated with plasma retinol (Figure 5F).

Hepatic Expression of Genes Involved in Vitamin A Storage, Transport, Hydrolysis, and Retinoic Acid-Responsive Targets Are Elevated in *ob/ob* Mice

Similar to HFC-fed mice, hepatic expression of *Lrat* and *Dgat1* was significantly enhanced in *ob/ob* mice as compared with controls, while expression of *Dgat2* and *Rbp4* was not different between both animal groups (Figure 6A). *Pnpla3* was strongly enhanced in *ob/ob* mice compared with control mice, while *Pnpla2* and *Lipe* levels were unchanged. In contrast to HFC-fed mice, *Raldh2* mRNA levels were reduced in *ob/ob* mice, while *Raldh1* and *Raldh3* levels were significantly elevated (Figure 6B). Finally, hepatic expression of various retinoic acid-responsive genes was also enhanced in *ob/ob* mice livers as compared with controls (Figure 6C). Taken together, both NAFLD mouse models present comparable impairments in hepatic vitamin A homeostasis.

Figure 1. (See previous page). Hepatic fat accumulation and steatohepatitis in HFC-fed mice. Mice fed chow or HFC diet for 12 or 20 weeks were analyzed for (A) body weight, (B) liver weight, (C) liver total cholesterol levels, (D) liver triglyceride (TG) levels, (E) liver free cholesterol levels, (F) plasma total cholesterol levels, (G) plasma free cholesterol levels, (H) plasma insulin levels, and (I) hematoxylin and eosin (H&E) staining, Oil Red O staining, and CD68 immunohistochemistry. Quantification of (immuno)histochemistry is described in the Methods and Materials. * $P \leq .05$, ** $P \leq .01$, *** $P \leq .001$.

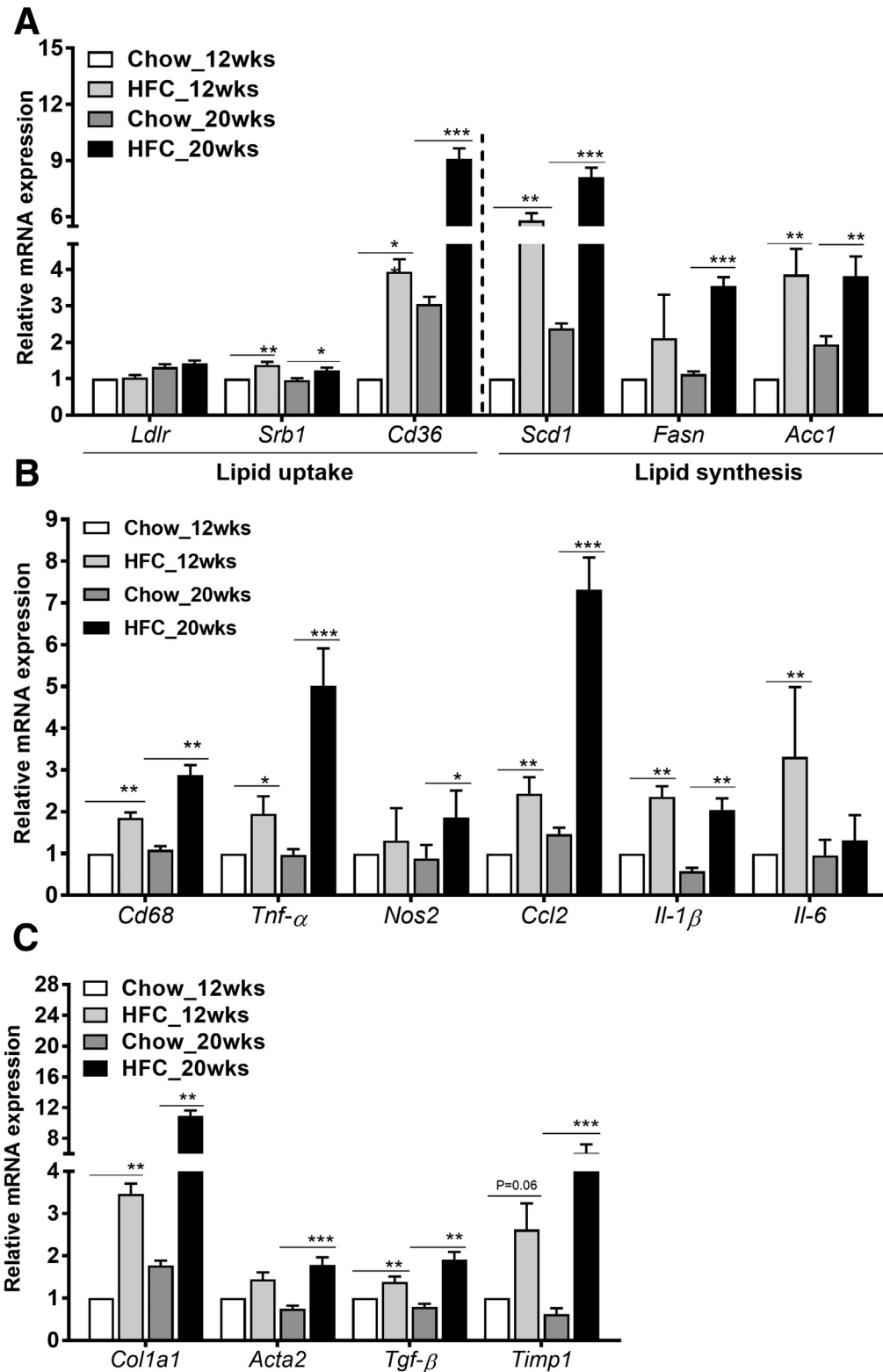


Figure 2. Expression of hepatic genes involved in lipid uptake, lipid synthesis, inflammation, and fibrosis in HFC-fed mice. Mice fed chow or HFC diet for 12 or 20 weeks were analyzed by Q-PCR for hepatic expression of genes involved in (A) hepatic lipid uptake (*Srb1*, *Cd36*) and synthesis (*Scd1*, *Fasn*, *Acc1*), (B) hepatic inflammation (*Cd68*, *Tnf- α* , *Nos2*, *Ccl2*, *Il-1 β* , *Il-6*), and (C) liver fibrosis (*Coll1a1*, *Acta2*, *Tgf- β* , and *Timp1*). Hepatic lipid uptake and synthesis, hepatic inflammation, and hepatic fibrosis were strongly increased in HFC-fed mice. * $P \leq .05$, ** $P \leq .01$, *** $P \leq .001$.

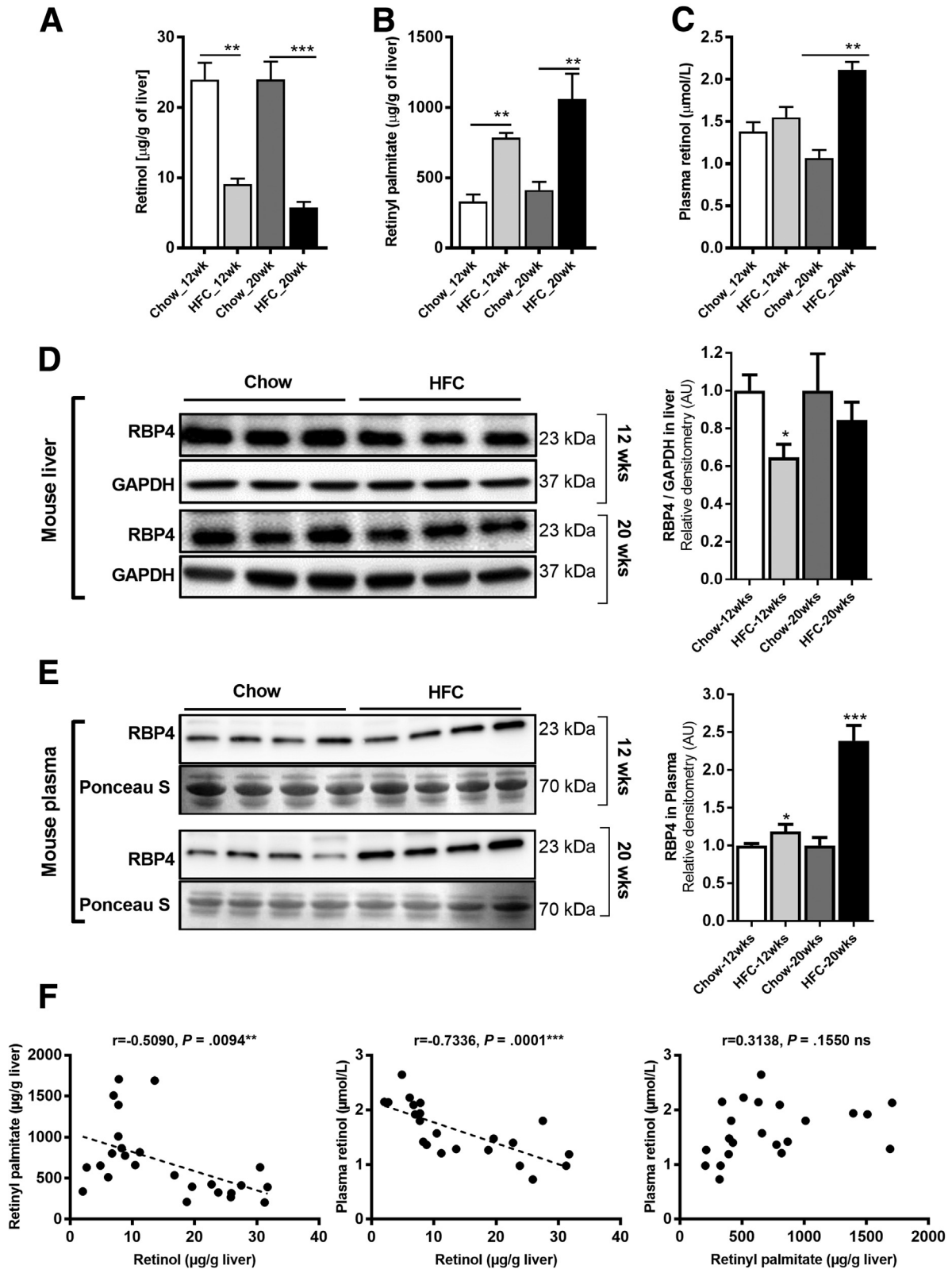


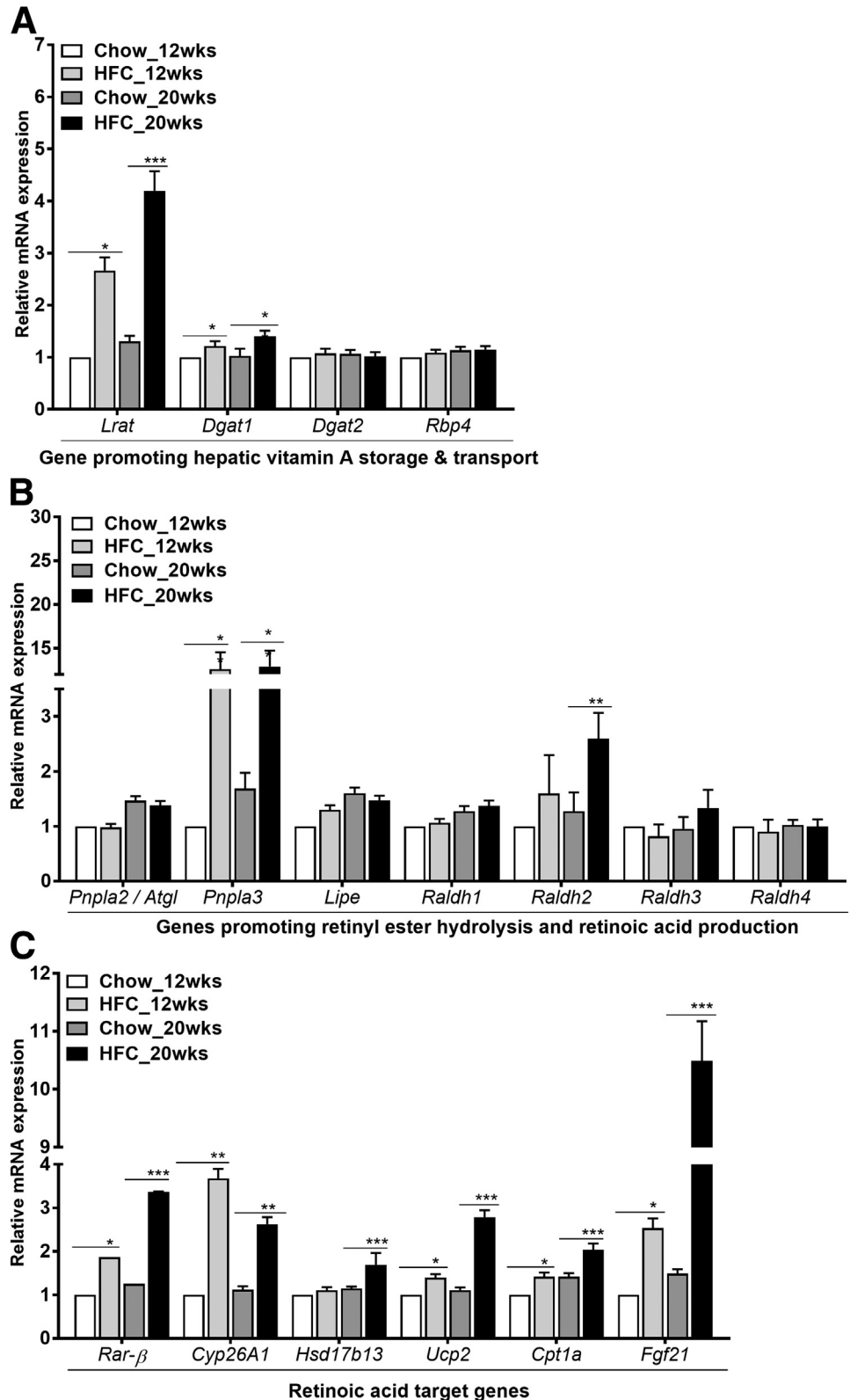
Figure 3. An HFC diet leads to impaired hepatic vitamin A metabolism in mice. Mice fed chow or HFC diet for 12 or 20 weeks were analyzed for hepatic levels of (A) retinol, (B) retinyl palmitate, and (C) plasma levels of retinol. Hepatic retinol levels were strongly reduced in HFC-fed mice, while retinyl palmitate levels were significantly increased compared with control mice. Twelve-week HFC-feeding did not alter plasma retinol levels, which were slightly elevated after 20 weeks. (D) Hepatic RBP4 protein levels were decreased in 12 week HFC-fed mice, while this decrease was no longer significant after 20 week HFC feeding. (E) Plasma RBP4 progressively increased in HFC-fed mice. (F) Correlation analysis of hepatic vitamin A (retinol, retinyl palmitate) with circulatory vitamin A (plasma retinol). * $P \leq .05$, ** $P \leq .01$, *** $P \leq .001$.

Palmitate Increases *Lrat* Expression and Vitamin A Accumulation in Primary Rat Hepatocytes

Dietary vitamin A is absorbed by hepatocytes through retinyl ester-carrying chylomicron remnants, after which it is redistributed to HSCs for storage (see Introduction). Thus,

both hepatocytes and HSCs are possible sites for retinyl ester accumulation, and earlier work has suggested vitamin A accumulation in hepatocytes of human and rodent fatty livers.^{18,19} Microscopical analysis of liver tissue for vitamin A-specific autofluorescence revealed few bright (auto)

Figure 4. Hepatic expression of genes involved in vitamin A homeostasis is strongly affected in HFC-fed mice. Mice fed chow or HFC diet for 12 or 20 weeks were analyzed by Q-PCR for hepatic expression of genes and transcription factors involved in (A) vitamin A storage (*Lrat*, *Dgat1*, *Dgat2*) and transport (*Rbp4*), (B) retinyl ester hydrolysis (*Atgl/Pnpla2*, *Pnpla3*, *Lipe*) and retinol-to-retinoic acid conversion (*Raldh1*, *Raldh2*, *Raldh3*, *Raldh4*), and (C) retinoic acid target genes (*Rar-β*, *Cyp26a1*, *Hsd17b13*, *Ucp2*, *Cpt1a*, *Fgf21*). Hepatic expression of vitamin A storage and hydrolysis were increased in HFC-fed mice, in conjunction with enhanced expression of retinoic acid responsive genes. * $P \leq .05$, ** $P \leq .01$, *** $P \leq .001$.



fluorescent dots in the hepatic parenchyme of chow-fed mice (Figure 7A, middle top panel) reminiscent of the distribution of quiescent HSCs and the pattern observed by

others in healthy rat and human livers.^{18,19} The autofluorescence signal strongly increased in livers of HFC-fed mice, showing a completely altered staining pattern, which

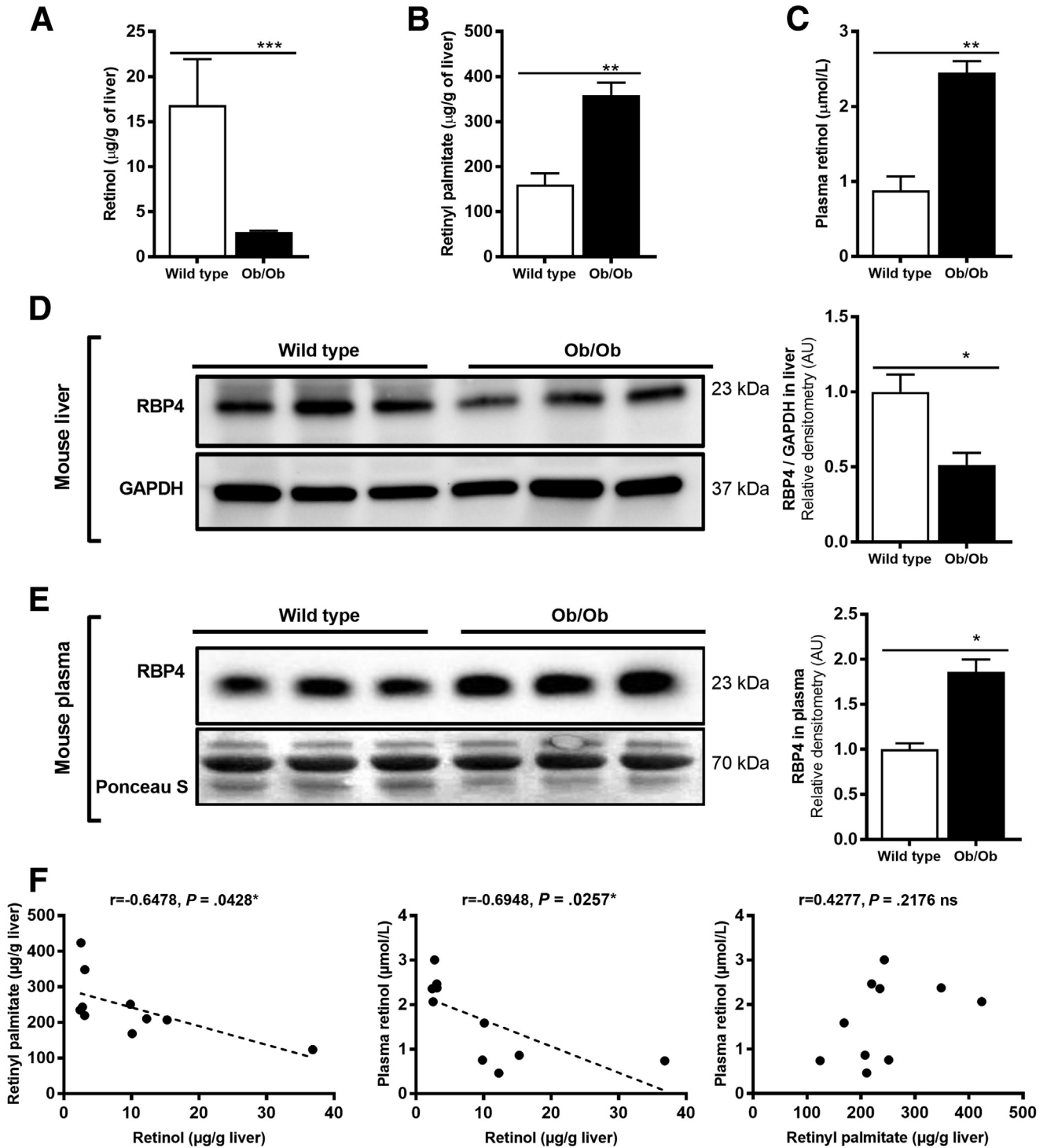


Figure 5. *Ob/ob* mice show disturbed hepatic vitamin A metabolism. *Ob/ob* mice and age-matched wild-type littermates were sacrificed and analyzed for (A) hepatic retinol, (B) hepatic retinyl palmitate, (C) plasma retinol, and (D) hepatic and (E) plasma RBP4 levels. Hepatic retinol levels were strongly reduced, while retinyl palmitate levels were significantly increased in *ob/ob* mice. Plasma retinol and RBP4 protein levels were significantly elevated in *ob/ob* mice. In contrast, hepatic RBP4 protein levels were reduced. Note that hepatic RBP4 mRNA levels were not changed in *ob/ob* mice (see Figure 6A). (F) Correlation analysis of hepatic vitamin A (retinol, retinyl palmitate) with circulatory vitamin A (plasma retinol). $*P \leq .05$, $**P \leq .01$, $***P \leq .001$.

now appeared in large vesicular structures (“lipid droplets”) that localize predominantly in hepatocytes (Figure 7A, middle bottom panel; the Oil Red O staining for lipids is shown in the left panels for comparison). Immunohistochemical analysis of cell type-specific expression of hepatic LRAT revealed that it was predominantly present in (quiescent) HSCs in chow-fed mice (Figure 7A, top right panel) and remained undetectable in hepatocytes. In contrast, LRAT-specific staining was readily detected in hepatocytes in HFC-fed mice (Figure 7A, bottom right panel).

In order to study cell type-specific effects of vitamin A storage in an *in vitro* model of fatty liver disease, we exposed primary rat hepatocytes, as well as quiescent and activated primary rat HSCs, to palmitate and found that it enhanced *Lrat* mRNA levels only in hepatocytes and not in quiescent HSCs (Figure 7B). Conversely, *Pnpla3* mRNA levels were elevated by palmitate exposure specifically in HSCs. Moreover, cellular retinyl palmitate levels significantly increased only in primary rat hepatocytes exposed to palmitate together with retinol for 48 hours (Figure 7C).

These results suggest that NAFLD promotes vitamin A loss in HSCs while vitamin A storage is induced in hepatocytes.

Discussion

In this study, we show that steatohepatitis in mice heavily affects hepatic vitamin A metabolism, leading to reduced retinol and enhanced retinyl ester levels in the liver. Notably, retinyl esters accumulate in hepatocytes rather than in HSCs, cells that store vitamin A esters in a healthy liver. Following retinol levels, hepatic RBP4 levels are also reduced, while increased in circulation. Thus, steatohepatitis does not lead to true vitamin A deficiency as suggested by earlier studies, but rather leads to hepatic retinol deficiency due to metabolic changes. Vitamin A supplementation in the form of retinyl esters may therefore be counterproductive in NAFLD, as it will likely accumulate in the already overloaded hepatocytes. Also, aberrant vitamin A metabolism may directly affect the activity of nuclear receptors, such as RAR, PPARs, LXR, and FXR, as they require RXR for most of their actions.

Chronic liver diseases, including NAFLD, are associated with low serum and hepatic retinol levels, which is generally considered to be a sign of systemic vitamin A deficiency.^{10,11,20–22} Moreover, serum and hepatic retinol levels are negatively correlated with liver disease progression.^{10,20,23,24} However, systemic retinol levels are only a very small fraction of the total pool of vitamin A, which mostly consists of retinyl esters stored in liver ($\geq 80\%$) and adipose tissue (10%–20%).^{25,26} Thus, systemic retinol levels alone are not a reliable marker for hypovitaminosis A *per se*.

Available information about the hepatic levels of the various retinoids (retinyl esters, retinol and retinoic acids) in NAFLD patients and animal models of NAFLD is highly controversial. Recent studies suggested that levels of all retinoids are reduced in mouse and human NAFLD

livers,^{11,27} while earlier studies reported that NAFLD is associated with hepatic vitamin A accumulation in humans and rodents.^{18,19} Detailed knowledge about this is, however, crucial for patient care, as it will indicate whether vitamin A supplementation or therapy with specific vitamin A metabolites may have therapeutic value.

Our study largely confirms the reduction in hepatic retinol concentrations in fatty livers, as reported by others^{10,20,27,28} but reports the opposite effect for hepatic retinyl palmitate levels. Others reported that also retinyl palmitate levels in the livers of high-fat diet (HFD)-fed mice and *ob/ob* mice as well as human NAFLD were decreased.^{11,27} Several reasons may account for this discrepancy. First was HFD vs HFC diet: A high-fat (only) diet may affect vitamin A metabolism differently than the HFC diets used in this study. However, we did not detect a reduction in hepatic retinyl palmitate levels in mice fed an HFD for 12 weeks, while hepatic retinol levels were reduced in both HFD- and HFC-fed mice (Figure 3A and 8). Second was the amount of vitamin A in the diets: in our study, both the control chow and HFC diet contained equal amounts of vitamin A (eg, 20 IU/g). The earlier study¹¹ used an HFD that contained significantly less vitamin A compared with the control chow (3.8 vs 15 IU/g plus additional β -carotene, respectively). Dietary intake of vitamin A, even above daily recommendations, correlates directly with hepatic levels of retinyl palmitate and retinol.^{29–32} Thus, for establishing an effect of a (high-fat) diet on hepatic vitamin A metabolism, it is crucial to standardize the dietary vitamin A intake for control and experimental diet. This is the case in the *ob/ob* mouse studies and cannot explain the opposing results between our and the earlier study. Third, retinol/retinyl ester extraction procedure: extraction of retinol and retinyl esters from serum or tissue is typically performed with either *n*-hexane^{25,33} or acetonitrile,^{11,27} though this is not always specified in methods sections. We compared both methods and found that acetonitrile very inefficiently extracts retinyl palmitate specifically from fatty liver tissue, while retinol extraction was similar with these solvents (Figure 9). This suggests that the extraction of retinyl esters by acetonitrile is compromised when a lot of fat is present in the (liver) tissue. Especially this latter procedural finding may explain the controversial findings on retinyl ester levels in fatty livers.

We show that hepatic fat accumulation in mice is associated with a strong reduction in hepatic retinol levels, but not in circulation. This is in line with earlier observations^{10,11,20–22} and indicates that the mouse NAFLD models used do show the hepatic phenotype but do not replicate the reduced circulatory retinol levels observed in NAFLD patients.^{10,20,27,28} NAFLD mouse models likely reflect only the initiating phase of NAFLD, and serum retinol levels are also hardly affected at that stage in patients. Alternatively, the observed difference may be species related, but this requires analyses of vitamin A metabolism in more severe mouse NAFLD models. We did observe, however, that serum RBP4 levels are elevated in NAFLD mice, which is also found in obese individuals with or without established NAFLD.^{34–38} In contrast, hepatic RBP4 levels are reduced

in NAFLD mice. This implies that, even though hepatic retinol levels are low, sufficient retinol is produced to promote—and even enhance—RBP4 secretion from the liver. Efficient RBP4 secretion from the liver strongly

depends on retinol availability. Vitamin A deficiency leads to pronounced hepatic accumulation of retinol-free apo-RBP4 under unchanged *Rbp4* mRNA levels and is rapidly released into the circulation upon retinol or retinoic acid

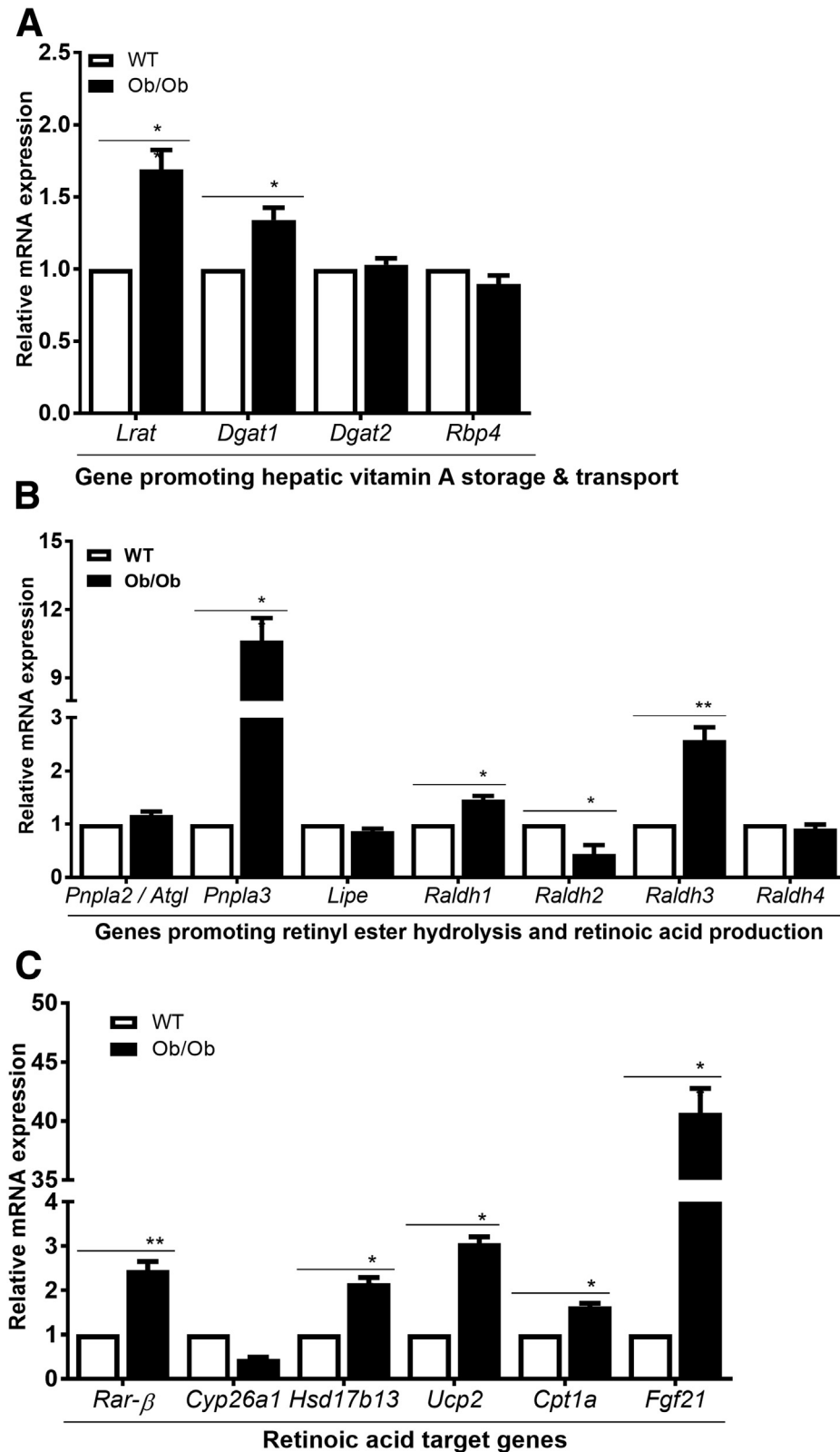


Figure 6. Hepatic expression of genes involved in vitamin A homeostasis is strongly affected in *ob/ob* mice. *Ob/ob* mice and age-matched wild-type (WT) littermates were sacrificed and analyzed by Q-PCR for hepatic expression of genes and transcription factors involved in (A) vitamin A storage (*Lrat*, *Dgat1*, *Dgat2*), transport (*Rbp4*), (B) vitamin A hydrolysis (*Atgl/Pnpla2*, *Pnpla3*, *Lipe*) and retinol-to-retinoic acid conversion (*Raldh1*, *Raldh2*, *Raldh3*, *Raldh4*), and (C) retinoic acid target genes (*Rar-β*, *Cyp26a1*, *Hsd17b13*, *Ucp2*, *Cpt1a*, *Fgf21*). Hepatic expression of vitamin A storage and hydrolysis was increased in *ob/ob*, in conjunction with enhanced expression of retinoic acid responsive genes. * $P \leq .05$, ** $P \leq .01$.

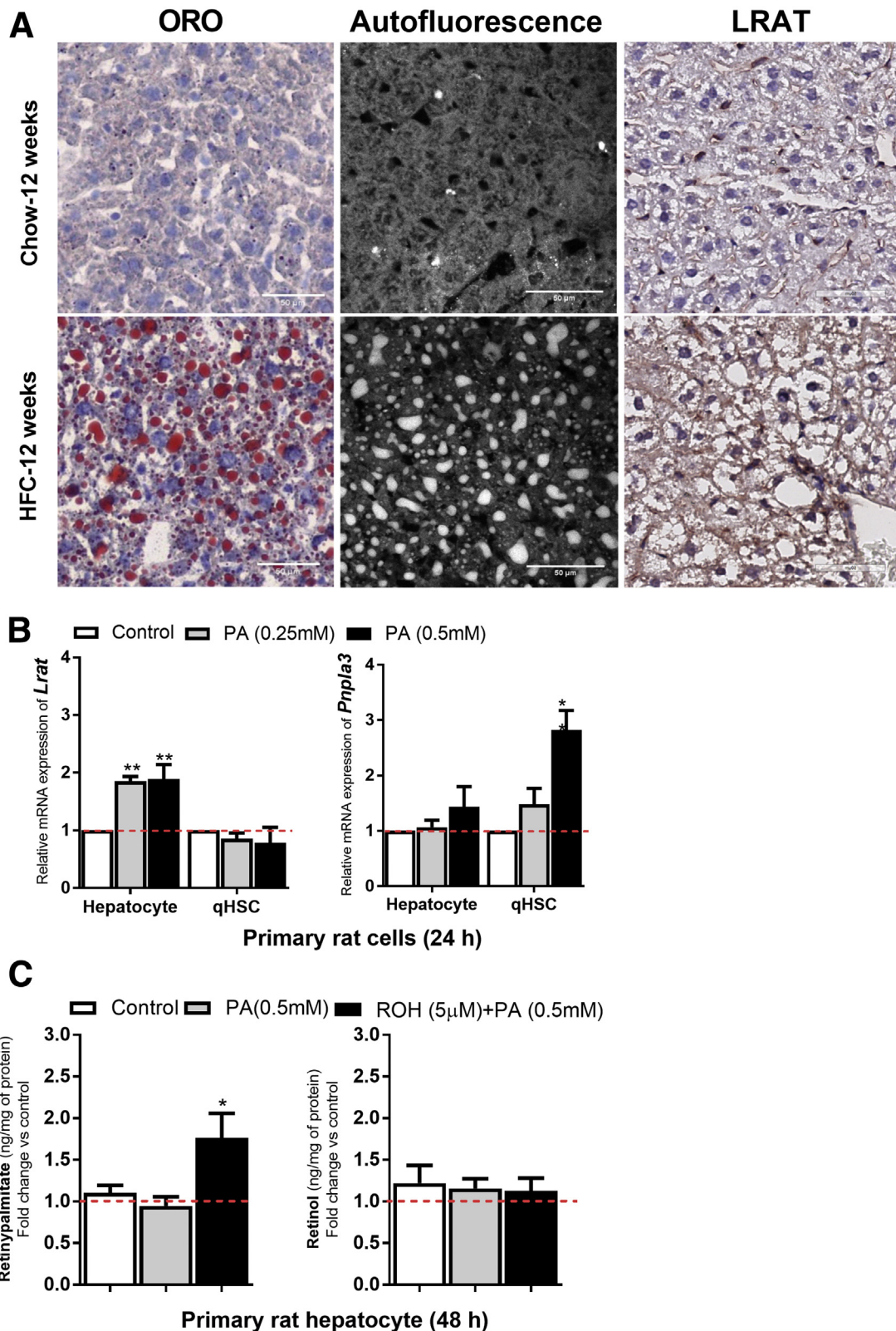


Figure 7. Accumulation of vitamin A in lipid-loaded hepatocytes in vivo and in vitro. (A) Oil Red O staining (left panels) and vitamin A-specific autofluorescence (middle panels) immunohistochemistry of LRAT (right panels) of liver sections of chow-fed (top panels) and HFC-fed (bottom panels) mice. Vitamin A-specific autofluorescence was strongly increased in livers of HFC-fed mice and was located predominantly in hepatocytes compared with its location in sparsely present HSCs in livers of chow-fed mice. (B) Freshly isolated and 4-hour attached primary rat hepatocytes and quiescent primary HSCs were and immediately treated with and without palmitate (PA) for 24 hours. Cells were harvested and analyzed by Q-PCR analysis for *Lrat* and *Pnpla3* expression. The gene expression is presented in $2^{-\Delta\Delta CT}$ and normalized to *18S*. (C) Freshly isolated and 4-hour attached primary rat hepatocytes were treated for 48 hours with and without PA and retinol (ROH), followed by analysis of cellular retinyl PA and ROH levels. * $P \leq .05$, ** $P \leq .01$.

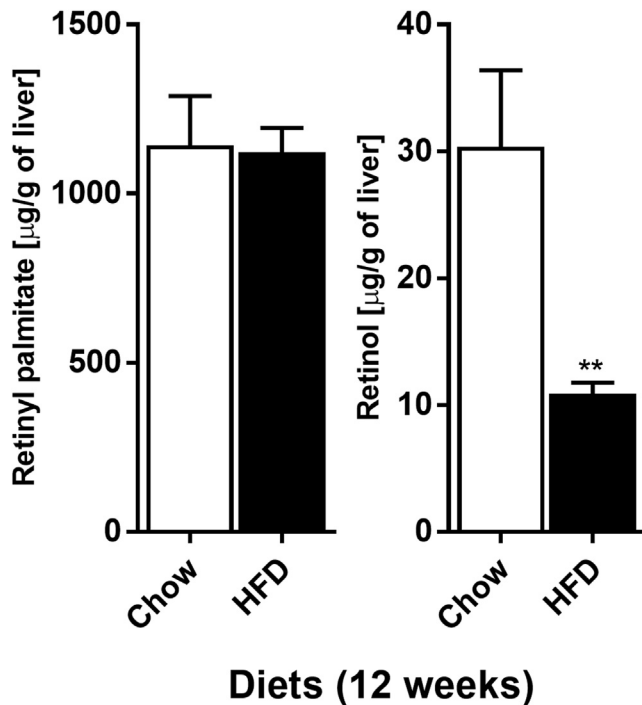


Figure 8. An HFD leads to impaired hepatic vitamin A metabolism in mice. Mice were fed a chow diet or HFD diet for 12 weeks and analyzed for hepatic levels of retinol hepatic levels of retinyl palmitate. Hepatic retinol levels were strongly reduced in HFD-fed mice as compared with control mice. However, hepatic retinyl palmitate levels did change in both groups. ** $P \leq .01$.

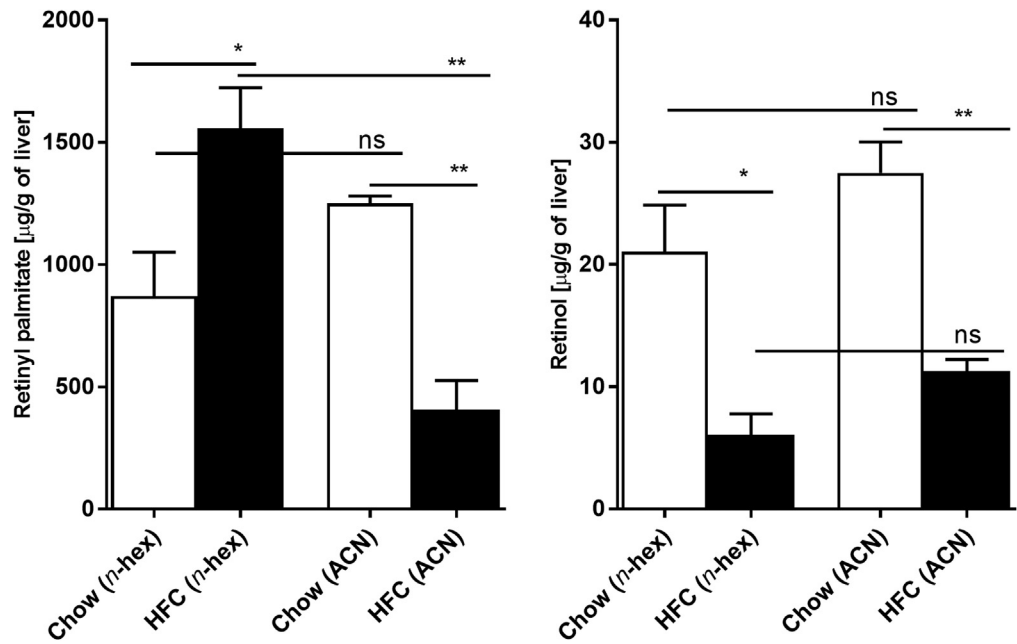
treatment.^{39–41} As hepatic retinol levels were low, enhanced RBP4 secretion may also result from enhanced production of retinoic acids. Indeed, mRNA levels of *Raldh1*, the main enzyme responsible for RA production in the liver, were significantly elevated in *ob/ob* mice, with similar trends observed for 12- and 20-week HFC-fed mice. A similar increase in *RALDH1* (*ALDH1A1*) expression in human nonalcoholic steatohepatitis liver was recently reported,²⁷ though retinoic acid levels were reduced, when compared with control livers. We observed a more general hepatic induction of RA-responsive genes in NAFLD mice, including *RAR- β* , *Cyp26a1*, *Hsd17b13*, *Ucp2*, *Cpt1a*, and *Fgf21*, which is in line with the earlier reported hypermetabolic state of hepatic vitamin A metabolism and degradation in NAFLD patients.¹⁴ It may be important now to establish whether the extraction efficiency of retinoic acids are also different using acetonitrile, used by Zhong et al²⁷ and many others, or *n*-hexane, as we observed for retinyl palmitate. Hepatic levels of *Lrat* and *Dgat1*, genes that encode enzymes that esterify retinol, were enhanced in NAFLD mice, observations also made in NAFLD patients.¹⁴ This coincides with a strong increase in hepatic retinyl palmitate levels in NAFLD mice, which is the main retinyl ester in both human and rodents.^{42,43} Particularly relevant is the apparent redistribution of vitamin A from HSCs in control livers to lipid-loaded hepatocytes in fatty livers. Retinyl esters are rapidly converted to retinol in the healthy liver. Accumulation of retinyl

esters in lipid-loaded hepatocytes may therefore result from decreased hydrolysis or increased esterification. On the one hand, expression of *Atgl/Pnpla2* (hydrolysis) was not changed, while both *Lrat* and *Dgat1* (esterification) were enhanced in mouse fatty livers, indicating a shift to vitamin A storage in retinyl esters. On the other hand, PNPLA3/ADPN is also able to hydrolyze retinyl esters⁴⁴ and its expression is strongly increased in mouse fatty liver, like in human NAFLD patients.⁴⁵ Still, *PNPLA3*'s main substrates are triglycerides that also strongly accumulate in mouse fatty liver. This implies that its activity cannot compensate for the build-up of triglycerides in hepatocytes, as observed for retinyl palmitate. Notably, *Lrat* expression was induced in primary rat hepatocytes exposed to palmitate and they accumulate retinyl palmitate when co-exposed to retinol. These conditions did not regulate *Lrat* expression in qHSCs, but rather enhance retinyl ester hydrolysis by increasing *PNPLA3* expression. These findings are in line with the shift in the main location of vitamin A to hepatocytes in fatty liver in mice (this study), rats,¹⁹ and humans.¹⁸ The redistribution of retinyl esters from HSCs to hepatocytes may also promote NAFLD-associated fibrosis, as differentiation of qHSCs to myofibroblasts is characterized by the loss of vitamin A-containing lipid droplets. In NAFLD, this apparently happens in conjunction with pronounced accumulation of retinyl esters in the liver, but then primarily in hepatocytes.

The mechanism(s) underlying the differential palmitate-mediated regulation of *Lrat* and *Pnpla3* in hepatocytes and HSCs remain(s) to be determined. Saturated fatty acids, such as palmitate, regulate various transcriptional pathways that can directly or indirectly influence (cell type-specific) hepatic vitamin A metabolism.⁴⁶ Hepatic de novo lipogenesis is under the primary transcriptional control of HFD and saturated fatty acids, such as palmitate, affect a multitude of transcription factors, including the sterol response element-binding protein-1c (SREBP-1c), carbohydrate response element-binding protein (ChREBP), CAAT/enhancer-binding protein- α or β (C/EBP α or β), hepatic nuclear factor-4 α (HNF-4 α), peroxisome proliferator-activated receptor α and γ (PPAR α and γ), chicken ovalbumin upstream promoter transcription factor (COUP-TF), forkhead box O (FOXO), cAMP regulatory element-binding protein (CREBP), and nuclear factor κ B.^{47–49} Indeed, *PNPLA3* expression is under the direct control of SREBP-1c and ChREBP,⁵⁰ and thus palmitate-induced SREBP-1c and ChREBP may enhance hepatic *PNPLA3* and thereby promote retinyl ester loss. It will be therefore interesting now to analyze the possible contribution of the various transcription factors to *Lrat* and *Pnpla3* regulation in hepatocytes and HSCs. Additionally, palmitate may induce general cellular responses, such as cellular endoplasmic reticulum stress, protein turnover, autophagy, mitochondrial dysfunction, and cell death⁴⁹ that may indirectly affect vitamin A metabolism.

Taken together, our study shows that fatty liver disease is associated with hepatic accumulation of retinyl esters and disturbed vitamin A metabolism. The latter condition likely modulates disease progression, as it was recently shown

Figure 9. Comparison *n*-hexane and acetonitrile extraction in the mice liver. Effect of 2 different methods of vitamin A extractions was analyzed: (1) *n*-hexane (*n*-hex) (used in this study) or (2) acetonitrile method (ACN) as previously described¹¹ from same mice livers fed a chow diet or HFC diet for 20 weeks ($n = 3$). Remarkably, both methods extracted a similar amount of retinol, but a significant less fraction of retinyl esters was extracted with ACN method. * $P \leq .05$, ** $P \leq .01$.



that even moderate changes in hepatic RA production significantly enhance hepatic lipid accumulation.⁵¹ Moreover, lipid metabolism is tightly controlled by various nuclear receptors, like PPARs, FXR, LXR, and RAR, ligands of which are in advanced clinical trial stages for the treatment of NAFLD.⁴⁶ All these factors require RXR as obligate partner and aberrant production of RXR-activating retinoids will affect nuclear receptor/RXR signaling. Further studies are needed to determine the impact of changed vitamin A metabolism in NAFLD on the therapeutic efficacy of these drug targets.

Materials and Methods

Animals

Animal experiments were approved by the Institutional Animal Care and Use Committee, University of Groningen, the Netherlands. Briefly, age- and sex-matched (8–10 weeks old) C57BL/6J mice were fed either regular chow or an HFC diet (containing 21% fat, with 45% calories from butterfat and 0.2% cholesterol; SAFE [Scientific Animal Food and Engineering], Villemoisson-sur-Orge, France) for a period of 12 or 20 weeks ($n = 8$), as reported previously.^{52,53} Both diets contained 20 IU of retinyl acetate/g as a source of vitamin A. *Leptin*^{ob} mutant (JAX ob/ob) mice (10–12 weeks old; Charles River Laboratories, Wilmington, MA) and appropriate controls (C57BL/6J) were also studied and received chow diet. Animals were kept in a pathogen-free environment with alternating dark-light cycles of 12 hours, and controlled temperature (20–24°C) and relative humidity (55 ± 15%) receiving food and water ad libitum. Animals were fasted 4 hours before sacrifice. Tissues were snap-frozen in liquid nitrogen or fixed in paraformaldehyde. Blood was collected by heart puncture.

Isolation and Culture of Primary Rat Hepatocytes and HSCs

Primary rat hepatocytes and HSCs were isolated from Wistar rats (Charles River Laboratories) and cultured as previously described.⁵⁴ Briefly, primary hepatocytes were isolated after 2-step collagenase perfusion (Sigma-Aldrich, St. Louis, MO).^{55,56} Cell viability >80% was determined by Trypan blue (Sigma-Aldrich). Primary hepatocytes were used after 4 hours of attachment on collagen-coated plates in William's E (Gibco by Life Technologies; Thermo Fisher Scientific, Bleiswijk, the Netherlands) medium with 10% fetal calf serum, 50- $\mu\text{g}/\text{mL}$ gentamycin, and 100-U/mL penicillin/streptomycin/amphotericin B. Primary rat HSCs were isolated after pronase (Merck, Amsterdam, the Netherlands) and collagenase-P (Roche, Almere, the Netherlands) perfusion and followed by Nycodenz (Axis-ShieldPOC; Oslo, Norway) density gradient centrifugation.⁵⁵ Primary hepatocytes and HSCs were exposed to bovine serum albumin-conjugated palmitic acid (0.25 or 0.5 mmol/L; Sigma-Aldrich), with or without 5- μM retinol (Sigma-Aldrich) for 24–48 hours as previously described.⁵⁷

Quantitative Real-Time Reverse-Transcription Polymerase Chain Reaction

Quantitative real-time reverse transcription polymerase chain reaction was performed as previously described.⁵⁸ Briefly, total RNA was isolated from tissue samples using TRIzol reagent according to supplier's instructions (Thermo Fisher Scientific). RNA quality and quantity were determined using a Nanodrop 2000c UV-vis spectrophotometer (Thermo Fisher Scientific). Complementary DNA was synthesized from 2.5 μg of RNA by using random nonamers and M-MLV reverse transcriptase (Thermo

Fisher Scientific). TaqMan primers and probes were designed using Primer Express 3.0.1 (Thermo Fisher Scientific) and are shown in [Supplementary Table 2](#). All target genes were amplified using the Q-PCR core kit master mix (Eurogentec, Maastricht, the Netherlands) on a 7900HT Fast Real-Time PCR system (Thermo Fisher Scientific). SDSV2.4.1 (Thermo Fisher Scientific) was used to analyze the data. Expression of genes is presented in $2^{-\Delta\text{CT}}$ and normalized to *36B4*.

Western Blot Analysis

Protein samples were prepared for Western blot analysis as described previously.⁵⁹ Protein concentrations were quantified using the Bio-Rad protein assay (Bio-Rad, Hercules, CA) with bovine serum albumin as standard. Equal amounts of protein were separated on Mini-PROTEAN TGX precast 4%–5% gradient gels (Bio-Rad) and transferred to nitrocellulose membranes using the Trans-Blot turbo transfer system (Bio-Rad). Primary antibodies (anti-RBP4, 1:2,000; #ab109193 [Abcam, Cambridge, United Kingdom] and anti-GAPDH, 1:40,000 #CB1001 [Calbiochem; Merck-Millipore, Amsterdam-Zuidoost, the Netherlands]) and horseradish peroxidase-conjugated goat anti-rabbit secondary antibodies (1:2000; Agilent DAKO, Amstelveen, the Netherlands) were used for detection. Proteins were detected using the Pierce ECL Western blotting kit (Thermo Fisher Scientific). Images were captured using the chemidoc XRS system and Image Lab version 3.0 (Bio-Rad). The intensity of bands was quantified using ImageJ version 1.51 (National Institutes of Health, Bethesda, MD).

Histology and Pathological Scoring

Hematoxylin and eosin (hematoxylin and eosin) staining on liver sections (4 μm) was performed. Snap-frozen liver sections (5 μm) were stained using Oil Red O.^{60,61} A pathological score was calculated as previously described⁶² to determine the level of steatosis, as well as the grade of lobular inflammation.

Immunohistochemistry

Immunohistochemistry for CD68 (1:300; rabbit anti-mouse CD68; #137002; Biolegio, Nijmegen, the Netherlands) and LRAT (1:200 rabbit anti-mouse LRAT; #28075; Takara Immuno-Biological Laboratories, Gunma, Japan) was performed on snap-frozen liver sections as previously described.⁶³ Antigen retrieval was performed by microwave irradiation in citrate buffer, pH 6.0, and blocking of endogenous peroxidase with 0.3% H_2O_2 for 30 minutes. Horseradish peroxidase-conjugated goat anti-rabbit antibodies (1:50; #170-6515; Bio-Rad) was used as secondary antibody. Slides were stained with DAB for 10 minutes and hematoxylin was used as a counter nuclear stain (2 minutes at room temperature). Finally, slides were dehydrated and mounted with Eukitt (Sigma-Aldrich). Slides were scanned using a nanozoomer 2.0 HT digital slide scanner (C9600-12; Hamamatsu Photonics, Hamamatsu, Japan) and analyzed with Aperio ImageScope (version 11.1; Leica Microsystems,

Amsterdam, the Netherlands). CD68-positive cells were counted to assess the expansion of macrophages in the liver.

Lipid Analysis

Lipids were extracted from 15% (w/v) liver homogenate in phosphate-buffered saline by using the Bligh and Dyer method.⁶⁴ A colorimetric assay was used to determine total cholesterol (11489232; Roche Molecular Biochemicals, Almere, the Netherlands) and free cholesterol (113609910930; DiaSys Diagnostic Systems GmbH, Holzheim, Germany). Cholesterol standards (DiaSys Diagnostic Systems GmbH) were used as a reference. Triglycerides were quantified using the Trig/GB kit (1187771; Roche Molecular Biochemicals), and Roche Precimat Glycerol standards (16658800) were used as a reference.

Serum and Hepatic Vitamin A Analysis

Serum and tissue vitamin A content was analyzed by reverse-phase high-performance liquid chromatography as previously described.³³ Briefly, tissue (30–50 mg) was homogenized in phosphate-buffered saline to create a 15% (w/v) tissue homogenate. Then, tissue homogenate (66.70 μL equal to 10 mg of tissue) or serum (50 μL) were added in antioxidant mix (2.75 mL, containing 23.07-mmol/L pyrogallol, 1.32-mmol/L butylated hydroxytoluene, 5.83-mmol/L ethylenediaminetetraacetic acid, and 38.71-mmol/L ascorbic acid, dissolved in methanol:dH₂O [2.67:1], pH 5.4) and vortexed thoroughly for 1 minutes.

Retinol and retinyl esters were extracted and deproteinized twice with *n*-hexane in the presence of retinol acetate (100 μL , concentration 4 $\mu\text{mol/L}$) as an internal standard to assess the level of recovery after the extraction procedure. Standard curves created from a range of concentrations of retinol and retinyl palmitate were used to determine absolute tissue and serum concentrations of these compounds. Additionally, 2 negative controls (only containing internal standard) and 2 positive controls (low and high concentrations of retinol plus internal standard) were included in each series of extractions. Samples were evaporated under N_2 and diluted in 300- μL 100% ultra-pure ethanol. Then, 50 μL was injected in high-performance liquid chromatography (HT Separations Module 2795; Waters Alliance, East Lyme, CT) for phase separation on a C18 column (Waters Symmetry C18, dimension 150 \times 3.0 mm, particle size 5 μm ; Waters Corporation, Milford, MA) and measurement (UV-VIS, dual wavelength, UV-4075 Jasco, Tokyo, Japan). Retinoids in samples were identified by exact retention time of known standards in ultraviolet absorption at 325 nm by high-performance liquid chromatography. Finally, retinol and retinyl palmitate concentrations were calculated and normalized to final volume or tissue weight.

Vitamin A Autofluorescence in Liver Tissue

Autofluorescence analysis was performed on unstained cryostatic liver sections using a Zeiss LSM 780 NLO 2-

photon CLSM (Carl Zeiss, Jena, Germany) as previously described.^{18,65} Briefly, cryostat liver sections were illuminated with an excitation filter of 366-nm band-pass interference, and spectra were recorded in the range of 400–680 nm with spectrum acquisition from 0.2 to 3 seconds.

Statistical Analysis

Data is presented in group mean \pm SEM and statistical analysis was performed using the GraphPad Prism 6 software package (GraphPad Software, San Diego, CA). Statistical significance was determined by Mann-Whitney test (2 groups), One-way analysis of variance or Kruskal-Wallis (more than 2 groups) followed by post hoc Dunn's test (compare all pairs of columns). Pearson correlation was performed between tissue and circulatory vitamin A with various parameters of NAFLD progression.

References

- Albhaisi S, Sanyal A. Recent advances in understanding and managing non-alcoholic fatty liver disease. *F1000Res* 2018; 7F1000 Faculty Rev-720.
- Bellentani S, Scaglioni F, Marino M, Bedogni G. Epidemiology of non-alcoholic fatty liver disease. *Dig Dis* 2010;28:155–161.
- Katsagoni CN, Georgoulis M, Papatheodoridis GV, Panagiotakos DB, Kontogianni MD. Effects of lifestyle interventions on clinical characteristics of patients with non-alcoholic fatty liver disease: a meta-analysis. *Metabolism* 2017;68:119–132.
- Iredale JP, Thompson A, Henderson NC. Extracellular matrix degradation in liver fibrosis: biochemistry and regulation. *Biochim Biophys Acta* 2013;1832:876–883.
- Schreiber R, Taschler U, Preiss-Landl K, Wongsiriroj N, Zimmermann R, Lass A. Retinyl ester hydrolases and their roles in vitamin A homeostasis. *Biochim Biophys Acta* 2012;1821:113–123.
- Blaner WS, O'Byrne SM, Wongsiriroj N, Kluwe J, D'Ambrosio DM, Jiang H, Schwabe RF, Hillman EMC, Piantadosi R, Libien J. Hepatic stellate cell lipid droplets: a specialized lipid droplet for retinoid storage. *Biochim Biophys Acta* 2009;1791:467–473.
- Senoo H, Mezaki Y, Fujiwara M. The stellate cell system (vitamin A-storing cell system). *Anat Sci Int* 2017; 92:387–455.
- Saeed A, Hoekstra M, Hoeke MO, Heegsma J, Faber KN. The interrelationship between bile acid and vitamin A homeostasis. *Biochim Biophys Acta* 2017; 1862:496–512.
- Brown E, Akré J, eds. Indicators for assessing vitamin A deficiency and their application in monitoring and evaluating intervention programmes. Geneva, Switzerland: World Health Organization, 1996.
- Chaves GV, Pereira SE, Saboya CJ, Spitz D, Rodrigues CS, Ramalho A. Association between liver vitamin A reserves and severity of nonalcoholic fatty liver disease in the class III obese following bariatric surgery. *Obes Surg* 2014;24:219–224.
- Trasino SE, Tang X-H, Jessurun J, Gudas LJ. Obesity leads to tissue, but not serum vitamin A deficiency. *Sci Rep* 2015;5:15893.
- Kovarova M, Königsrainer I, Königsrainer A, Machicao F, Häring H-U, Schleicher E, Peter A. The genetic variant I148M in PNPLA3 is associated with increased hepatic retinyl-palmitate storage in humans. *J Clin Endocrinol Metab* 2015;100:E1568–E1574.
- Ma Y, Belyaeva OV, Brown PM, Fujita K, Valles K, Karki S, de Boer YS, Koh C, Chen Y, Du X, Handelman SK, Chen V, Speliotes EK, Nestlerode C, Thomas E, Kleiner DE, Zmuda JM, Sanyal AJ, (for the Nonalcoholic Steatohepatitis Clinical Research Network), Kedishvili NY, Liang TJ, Rotman Y. 17-Beta hydroxysteroid dehydrogenase 13 is a hepatic retinoid dehydrogenase associated with histological features of nonalcoholic fatty liver disease. *Hepatology* 2019; 69:1504–1519.
- Ashla AA, Hoshikawa Y, Tsuchiya H, Hashiguchi K, Enjoji M, Nakamuta M, Taketomi A, Maehara Y, Shomori K, Kurimasa A, Hisatome I, Ito H, Shiota G. Genetic analysis of expression profile involved in retinoid metabolism in non-alcoholic fatty liver disease. *Hepato Res* 2010;40:594–604.
- Makia NL, Bojang P, Falkner KC, Conklin DJ, Prough RA. Murine hepatic aldehyde dehydrogenase 1a1 is a major contributor to oxidation of aldehydes formed by lipid peroxidation. *Chem Biol Interact* 2011;191:278–287.
- Kathmann EC, Naylor S, Lipsky JJ. Rat liver constitutive and phenobarbital-inducible cytosolic aldehyde dehydrogenases are highly homologous proteins that function as distinct isozymes. *Biochemistry* 2000; 39:11170–11176.
- Bhatt DK, Gaedigk A, Pearce RE, Leeder JS, Prasad B. Age-dependent protein abundance of cytosolic alcohol and aldehyde dehydrogenases in human liver. *Drug Metab Dispos* 2017;45:1044–1048.
- Croce AC, De Simone U, Freitas I, Boncompagni E, Neri D, Cillo U, Bottiroli G. Human liver autofluorescence: an intrinsic tissue parameter discriminating normal and diseased conditions. *Lasers Surg Med* 2010;42:371–378.
- Croce AC, Ferrigno A, Piccolini VM, Tarantola E, Boncompagni E, Bertone V, Milanese G, Freitas I, Vairetti M, Bottiroli G. Integrated autofluorescence characterization of a modified-diet liver model with accumulation of lipids and oxidative stress. *Biomed Res Int* 2014;2014:803491.
- Botella-Carretero JI, Balsa JA, Vázquez C, Peromingo R, Díaz-Enriquez M, Escobar-Morreale HF. Retinol and alpha-tocopherol in morbid obesity and nonalcoholic fatty liver disease. *Obes Surg* 2010;20:69–76.
- Havaladar PV, Patel VD, Siddibhavi BM. Recurrent vitamin A deficiency and fatty liver. *J Trop Pediatr* 1991;37:87–88.
- Liu Y, Chen H, Wang J, Zhou W, Sun R, Xia M. Association of serum retinoic acid with hepatic steatosis and liver injury in nonalcoholic fatty liver disease. *Am J Clin Nutr* 2015;102:130–137.
- de Souza Valente da Silva L, Valeria da Veiga G, Ramalho RA. Association of serum concentrations of

- retinol and carotenoids with overweight in children and adolescents. *Nutrition* 2007;23:392–397.
24. Neuhouser ML, Rock CL, Eldridge AL, Kristal AR, Patterson RE, Cooper DA, Neumark-Sztainer D, Cheskin LJ, Thornquist MD. Serum concentrations of retinol, alpha-tocopherol and the carotenoids are influenced by diet, race and obesity in a sample of healthy adolescents. *J Nutr* 2001;131:2184–2191.
 25. Kane MA, Folias AE, Napoli JL. HPLC/UV quantitation of retinal, retinol, and retinyl esters in serum and tissues. *Anal Biochem* 2008;378:71–79.
 26. Blaner WS, Li Y, Brun P-J, Yuen JJ, Lee S-A, Clugston RD. Vitamin A absorption, storage and mobilization. *Subcell Biochem* 2016;81:95–125.
 27. Zhong G, Kirkwood J, Won K-J, Tjota N, Jeong H, Isoherranen N. Characterization of vitamin A metabolome in human livers with and without nonalcoholic fatty liver disease. *J Pharmacol Exp Ther* 2019;370:92–103.
 28. Suano de Souza FI, Silverio Amancio OM, Saccardo Sarni RO, Sacchi Pitta T, Fernandes AP, Affonso Fonseca FL, Hix S, Ramalho RA. Non-alcoholic fatty liver disease in overweight children and its relationship with retinol serum levels. *Int J Vitam Nutr Res* 2008;78:27–32.
 29. Sundaresan PR, Kaup SM, Wiesenfeld PW, Chirtel SJ, Hight SC, Rader JI. Interactions in indices of vitamin A, zinc and copper status when these nutrients are fed to rats at adequate and increased levels. *Br J Nutr* 1996;75:915–928.
 30. Johansson I, Hallmans G, Wikman A, Biessy C, Riboli E, Kaaks R. Validation and calibration of food-frequency questionnaire measurements in the Northern Sweden Health and Disease cohort. *Public Health Nutr* 2002;5:487–496.
 31. Cifelli CJ, Ross AC. Chronic vitamin A status and acute repletion with retinyl palmitate are determinants of the distribution and catabolism of all-trans-retinoic acid in rats. *J Nutr* 2007;137:63–70.
 32. Olivares A, Daza A, Rey AI, López-Bote CJ. Dietary vitamin A concentration alters fatty acid composition in pigs. *Meat Sci* 2009;81:295–299.
 33. Kim Y-K, Quadro L. Reverse-phase high-performance liquid chromatography (HPLC) analysis of retinol and retinyl esters in mouse serum and tissues. *Methods Mol Biol* 2010;652:263–275.
 34. Yang Q, Graham TE, Mody N, Preitner F, Peroni OD, Zabolotny JM, Kotani K, Quadro L, Kahn BB. Serum retinol binding protein 4 contributes to insulin resistance in obesity and type 2 diabetes. *Nature* 2005;436:356–362.
 35. Haider DG, Schindler K, Prager G, Bohdjalian A, Luger A, Wolzt M, Ludvik B. Serum retinol-binding protein 4 is reduced after weight loss in morbidly obese subjects. *J Clin Endocrinol Metab* 2007;92:1168–1171.
 36. Reinehr T, Stoffel-Wagner B, Roth CL. Retinol-binding protein 4 and its relation to insulin resistance in obese children before and after weight loss. *J Clin Endocrinol Metab* 2008;93:2287–2293.
 37. Tajtáková M, Semanová Z, Ivancová G, Petrovicová J, Donicová V, Zemberová E. [Serum level of retinol-binding protein 4 in obese patients with insulin resistance and in patients with type 2 diabetes treated with metformin]. *Vnitr Lek* 2007;53:960–963.
 38. Ulgen F, Herder C, Kühn MC, Willenberg HS, Schott M, Scherbaum WA, Schinner S. Association of serum levels of retinol-binding protein 4 with male sex but not with insulin resistance in obese patients. *Arch Physiol Biochem* 2010;116:57–62.
 39. Ronne H, Ocklind C, Wiman K, Rask L, Obrink B, Peterson PA. Ligand-dependent regulation of intracellular protein transport: effect of vitamin a on the secretion of the retinol-binding protein. *J Cell Biol* 1983;96:907–910.
 40. Dixon JL, Goodman DS. Studies on the metabolism of retinol-binding protein by primary hepatocytes from retinol-deficient rats. *J Cell Physiol* 1987;130:14–20.
 41. Bellovino D, Lanyau Y, Garaguso I, Amicone L, Cavallari C, Tripodi M, Gaetani S. MMH cells: An in vitro model for the study of retinol-binding protein secretion regulated by retinol. *J Cell Physiol* 1999;181:24–32.
 42. Futterman S, Andrews JS. The composition of liver vitamin A ester and the synthesis of vitamin A ester by liver microsomes. *J Biol Chem* 1964;239:4077–4080.
 43. Schäffer MW, Roy SS, Mukherjee S, Nohr D, Wolter M, Biesalski HK, Ong DE, Das SK. Qualitative and quantitative analysis of retinol, retinyl esters, tocopherols and selected carotenoids out of various internal organs from different species by HPLC. *Anal Methods* 2010;2:1320–1332.
 44. Pirazzi C, Valenti L, Motta BM, Pingitore P, Hedfalk K, Mancina RM, Burza MA, Indiveri C, Ferro Y, Montalcini T, Maglio C, Dongiovanni P, Fargion S, Rametta R, Pujia A, Andersson L, Ghosal S, Levin M, Wiklund O, Iacovino M, Borén J, Romeo S. PNPLA3 has retinyl-palmitate lipase activity in human hepatic stellate cells. *Hum Mol Genet* 2014;23:4077–4085.
 45. Aragonès G, Auguet T, Armengol S, Berlanga A, Guiu-Jurado E, Aguilar C, Martínez S, Sabench F, Porrás JA, Ruiz MD, Hernández M, Sirvent JJ, Del Castillo D, Richart C. PNPLA3 expression is related to liver steatosis in morbidly obese women with non-alcoholic fatty liver disease. *Int J Mol Sci* 2016;17:630.
 46. Saeed A, Dullaart RPF, Schreuder TCMA, Blokzijl H, Faber KN. Disturbed vitamin A metabolism in non-alcoholic fatty liver disease (NAFLD). *Nutrients* 2018;10:29.
 47. Xu C, Chakravarty K, Kong X, Tuy TT, Arinze IJ, Bone F, Massillon D. Several transcription factors are recruited to the glucose-6-phosphatase gene promoter in response to palmitate in rat hepatocytes and H4IIE cells. *J Nutr* 2007;137:554–559.
 48. Zhao N, Li X, Feng Y, Han J, Feng Z, Li X, Wen Y. The nuclear orphan receptor Nur77 alleviates palmitate-induced fat accumulation by down-regulating G0S2 in HepG2 cells. *Sci Rep* 2018;8:4809.
 49. Piccolis M, Bond LM, Kampmann M, Pulimeno P, Chittraju C, Jayson CBK, Vaites LP, Boland S, Lai ZW, Gabriel KR, Elliott SD, Paulo JA, Harper JW, Weissman JS, Walther TC, Farese RV. Probing the global cellular responses to lipotoxicity caused by saturated fatty acids. *Mol Cell* 2019;74:32–44.e8.

50. Dubuquoy C, Robichon C, Lasnier F, Langlois C, Dugail I, Fougelle F, Girard J, Burnol A-F, Postic C, Moldes M. Distinct regulation of adiponutrin/PNPLA3 gene expression by the transcription factors ChREBP and SREBP1c in mouse and human hepatocytes. *J Hepatol* 2011;55:145–153.
51. Yang D, Vuckovic MG, Smullin CP, Kim M, Pui-See Lo C, Devericks E, Yoo HS, Tintcheva M, Deng Y, Napoli JL. Modest decreases in endogenous all-trans-retinoic acid produced by a mouse *Rdh10* heterozygote provoke major abnormalities in adipogenesis and lipid metabolism. *Diabetes* 2018;67:662–673.
52. Bartuzi P, Wijshake T, Dekker DC, Fedoseienko A, Kloosterhuis NJ, Youssef SA, Li H, Shiri-Sverdlov R, Kuivenhoven J-A, de Bruin A, Burstein E, Hofker MH, van de Sluis B. A cell-type-specific role for murine *Commd1* in liver inflammation. *Biochim Biophys Acta* 2014;1842:2257–2265.
53. Bartuzi P, Billadeau DD, Favier R, Rong S, Dekker D, Fedoseienko A, Fieten H, Wijers M, Levels JH, Huijckman N, Kloosterhuis N, van der Molen H, Brufau G, Groen AK, Elliott AM, Kuivenhoven JA, Plecko B, Grangl G, McGaughan J, Horton JD, Burstein E, Hofker MH, van de Sluis B. CCC- and WASH-mediated endosomal sorting of LDLR is required for normal clearance of circulating LDL. *Nat Commun* 2016;7:10961.
54. Shajari S, Laliena A, Heegsma J, Tuñón MJ, Moshage H, Faber KN. Melatonin suppresses activation of hepatic stellate cells through $ROR\alpha$ -mediated inhibition of 5-lipoxygenase. *J Pineal Res* 2015;59:391–401.
55. Shajari S, Saeed A, Smith-Cortinez NF, Heegsma J, Sydor S, Faber KN. Hormone-sensitive lipase is a retinyl ester hydrolase in human and rat quiescent hepatic stellate cells. *Biochim Biophys Acta Mol Cell Biol Lipids* 2019;1864:1258–1267.
56. Woudenberg-Vrenken TE, Buist-Homan M, Conde de la Rosa L, Faber KN, Moshage H. Anti-oxidants do not prevent bile acid-induced cell death in rat hepatocytes. *Liver Int* 2010;30:1511–1521.
57. Song YM, Song S-O, Jung Y-K, Kang E-S, Cha BS, Lee HC, Lee B-W. Dimethyl sulfoxide reduces hepatocellular lipid accumulation through autophagy induction. *Autophagy* 2012;8:1085–1097.
58. Blokzijl H, Vander Borgh S, Bok LIH, Libbrecht L, Geuken M, van den Heuvel FAJ, Dijkstra G, Roskams TAD, Moshage H, Jansen PLM, Faber KN. Decreased P-glycoprotein (P-gp/MDR1) expression in inflamed human intestinal epithelium is independent of PXR protein levels. *Inflamm Bowel Dis* 2007;13:710–720.
59. Pellicoro A, van den Heuvel FAJ, Geuken M, Moshage H, Jansen PLM, Faber KN. Human and rat bile acid-CoA: amino acid N-acyltransferase are liver-specific peroxisomal enzymes: implications for intracellular bile salt transport. *Hepatology* 2007;45:340–348.
60. Fischer AH, Jacobson KA, Rose J, Zeller R. Hematoxylin and eosin staining of tissue and cell sections. *CSH Protoc* 2008;2008, pdb.prot4986.
61. Mehlem A, Hagberg CE, Muhl L, Eriksson U, Falkevall A. Imaging of neutral lipids by oil red O for analyzing the metabolic status in health and disease. *Nat Protoc* 2013;8:1149–1154.
62. Kleiner DE, Brunt EM, Van Natta M, Behling C, Contos MJ, Cummings OW, Ferrell LD, Liu Y-C, Torbenson MS, Unalp-Arida A, Yeh M, McCullough AJ, Sanyal AJ; Nonalcoholic Steatohepatitis Clinical Research Network. Design and validation of a histological scoring system for nonalcoholic fatty liver disease. *Hepatology* 2005;41:1313–1321.
63. Aparicio-Vergara M, Hommelberg PPH, Schreurs M, Gruben N, Stienstra R, Shiri-Sverdlov R, Kloosterhuis NJ, de Bruin A, van de Sluis B, Koonen DPY, Hofker MH. Tumor necrosis factor receptor 1 gain-of-function mutation aggravates nonalcoholic fatty liver disease but does not cause insulin resistance in a murine model. *Hepatology* 2013;57:566–576.
64. Bligh EG, Dyer WJ. A rapid method of total lipid extraction and purification. *Can J Biochem Physiol* 1959;37:911–917.
65. Croce AC, De Simone U, Vairetti M, Ferrigno A, Boncompagni E, Freitas I, Bottiroli G. Liver autofluorescence properties in animal model under altered nutritional conditions. *Photochem Photobiol Sci* 2008;7:1046–1053.

Received October 3, 2019. Accepted July 16, 2020.

Correspondence

Address correspondence to: Klaas Nico Faber, PhD, Department Hepatology & Gastroenterology, University Medical Center Groningen, Hanzeplein 1, 9713 GZ Groningen, the Netherlands. e-mail: k.n.faber@umcg.nl; fax: +31(0)503619306; or Ali Saeed, PhD, Department Hepatology & Gastroenterology, University Medical Center Groningen, Hanzeplein 1, 9713 GZ Groningen, the Netherlands. e-mail: a.saeed@umcg.nl; fax: +31(0)503619306.

Acknowledgments

The authors want to acknowledge Tim Van Zutphen and Dicky Struik for providing samples of *ob/ob* mice.

CRedit Authorship Contributions

Ali Saeed (Conceptualization: Lead; Data curation: Lead; Formal analysis: Lead; Investigation: Lead; Methodology: Lead; Project administration: Lead; Software: Lead; Validation: Lead; Writing – original draft: Lead; Writing – review & editing: Lead)

Paulina Bartuzi (Data curation: Supporting; Validation: Supporting)
Janette Heegsma, MSc (Data curation: Supporting; Formal analysis: Supporting; Methodology: Equal; Validation: Supporting)

Daphne Dekker (Data curation: Supporting; Formal analysis: Supporting)
Niels Kloosterhuis (Data curation: Supporting; Formal analysis: Supporting)
Alain de Bruin (Formal analysis: Supporting; Investigation: Supporting; Methodology: Supporting; Validation: Supporting; Visualization: Supporting)

Johan W Jonker (Resources: Supporting; Validation: Supporting; Visualization: Supporting; Writing – review & editing: Supporting)

Bart van de Sluis (Data curation: Equal; Formal analysis: Equal; Funding acquisition: Equal; Investigation: Equal; Methodology: Supporting; Project administration: Equal; Resources: Equal; Supervision: Supporting; Validation: Equal; Visualization: Equal; Writing – review & editing: Equal)

Klaas Nico Faber (Conceptualization: Lead; Formal analysis: Equal; Funding acquisition: Lead; Investigation: Equal; Methodology: Equal; Project administration: Lead; Resources: Lead; Supervision: Lead; Validation: Lead; Visualization: Equal; Writing – review & editing: Equal)

Conflicts of Interest

The authors disclose no conflicts.

Funding

This work was supported by the Dutch Digestive Disease Foundation, grant numbers MWO 03-38 (to Klaas Nico Faber) and MWO 08-70 (to Klaas Nico Faber).

Supplementary Table 1. Pearson Correlation Analysis of Vitamin A With Various Parameters of NAFLD in Mice Fed High-Fat, High-Cholesterol Diet

	Retinol		Retinyl palmitate		Plasma retinol		Total cholesterol	
	r	P	r	P	r	P	r	P
Retinol	1.000							
Retinyl palmitate	-.5090 ^a	.0094 ^a	1.000					
Plasma retinol	-.8336 ^a	.0001 ^a	.3138	.155	1.000			
Total cholesterol	-.6705 ^a	.0002 ^a	.4537 ^b	.0227 ^b	.4132 ^b	.0447 ^b	1.000	
Free cholesterol	-.6163 ^a	.0023 ^a	.2172	.3316	.3996	.0654	.8713 ^b	<.0001 ^b
Triglycerides	-.7264 ^a	<.0001 ^a	.4399 ^b	.0357 ^b	.3746	.0858	.8338 ^b	<.0001 ^b
Plasma total cholesterol	-.8558 ^a	<.0001 ^a	.3956	.0557	.7992 ^b	<.0001 ^b	.7002 ^b	<.0001 ^b
Plasma free cholesterol	-.6987 ^a	.0001 ^a	.3970	.0547	.7933 ^b	<.0001 ^b	.6201 ^b	.0007 ^b
Plasma insulin	-.4819 ^a	.0199 ^a	.1850	.3981	.3288	.1352	.4454 ^b	.0257 ^b
<i>Ldlr</i>	-.3034	.1404	-.0385	.8552	.3247	.1216	.0712	.724
<i>Srb1</i>	-.4420 ^a	.0269 ^a	.3330	.1038	.2512	.2364	.6968 ^b	<.0001 ^b
<i>Cd36</i>	-.7852 ^a	<.0001 ^a	.4761 ^b	.0161 ^b	.8182 ^b	<.0001	.5167 ^b	.0058 ^b
<i>Scd1</i>	-.8337 ^a	<.0001 ^a	.4571 ^b	.0216 ^b	.7339 ^b	<.0001 ^b	.6488 ^b	.0003 ^b
<i>Fasn</i>	-.6557 ^a	.0004 ^a	.2310	.2666	.5699 ^b	.0036 ^b	.3909 ^b	.0438 ^b
<i>Acc1</i>	-.6317 ^a	.0007 ^a	.2304	.2679	.5549 ^b	.0049 ^b	.4235 ^b	.0277 ^b
<i>Tnfa</i>	-.6956 ^a	.0001 ^a	.2370	.2541	.8304 ^b	.0001 ^b	.5063 ^b	.0071 ^b
<i>Nos2</i>	-.5468 ^a	.0057 ^a	.3073	.1441	.6059 ^b	.0022 ^b	.3951 ^b	.0457 ^b
<i>Ccl2</i>	-.6086 ^a	.0012 ^a	.2781	.1784	.7633 ^b	<.0001 ^b	.4329 ^b	.0241 ^b
<i>Il1b</i>	-.6533 ^a	.0004 ^a	.4088 ^b	.0425 ^b	.3854	.0629	.6062 ^b	.0008 ^b
<i>Il6</i>	-.3023	.1511	.3158	.1327	.0613	.7863	.4628 ^b	.0198 ^b
<i>Co1a1</i>	-.6398 ^a	.0006 ^a	.1263	.5473	.7626 ^b	<.0001 ^b	.4320 ^b	.0244 ^b
<i>Acta2</i>	-.6355 ^a	.0006 ^a	.1773	.3965	.6210 ^b	.0012 ^b	.5299 ^b	.0045 ^b
<i>Tgfb</i>	-.7158 ^a	<.0001 ^a	.2572	.2145	.7649 ^b	<.0001 ^b	.6454 ^b	.0003 ^b
<i>Timp1</i>	-.5585 ^a	.0037 ^a	.0657	.7552	.7044 ^b	.0001 ^b	.3541	.07

Pearson correlation analysis of hepatic vitamin A (retinol, retinyl palmitate) with circulatory vitamin A (plasma retinol) with various parameters of diet-induced NAFLD progression. A correlation was also calculated between tissue and circulatory vitamin A with hepatic gene expression of markers for the progression of NAFLD. D $P \leq .05$ considered significant. NAFLD, nonalcoholic fatty liver disease.

^aSignificant inverse correlation.

^bPositive correlation.

Supplementary Table 2. Primers and Probes Used in Study for Analysis of Target Genes

Gene/ID	TaqMan primers and probe
<i>36B4</i> NM_022402	Fwd: 5'-GCTTCATTGTGGGAGCAGACA-3' Rev: 5'-CATGGTGTTCCTTGCCCATCAG-3' Probe: 5'-TCCAAGCAGATGCAGCAGATCCGC-3'
<i>Acaca/Acc1</i> NM_133360.1/NM_022193.1	Fwd: 5'-GCCATTGGTATTGGGGCTTAC-3' Rev: 5'-CCCGACCAAGGACTTTGTTG-3' Probe: 5'-CTCAACCTGGATGGTCTTTGTCCCAGC-3'
<i>Act2/α-Sma</i> NM_007392	Fwd: 5'-TTCGTGTGGCCCTGAAG-3' Rev: 5'-GGACAGCACAGCCTGAATAGC-3' Probe: 5'-TTGAGACCTTCAATGTCCCCGCCA-3'
<i>Cd36</i> BC010262/NM_031561	Fwd: 5'-GATCGGAACTGTGGGCTCAT-3' Rev: 5'-GGTTCCTTCTTCAAGGACAACCTC-3' Probe: 5'-AGAATGCCTCCAAACACAGCCAGGAC-3'
<i>Cd68</i> NM_009853	Fwd: 5'-CACTTCGGGCCATGTTTCTC-3' Rev: 5'-AGGACCAGGCCAATGATGAG-3' Probe: 5'-CAACCGTGACCAGTCCCTCTTGCTG-3'
<i>Ccl2</i> NM_031530.1	Fwd: 5'-TGTCTCAGCCAGATGCAGTTAAT-3' Rev: 5'-CCGACTCATTGGGATCATCTT-3' Probe: 5'-CCCCACTCACCTGCTGCTACTCATTCA-3'
<i>Col1a1</i> NM_007742	Fwd: 5'-TGGTGAACGTGGTGTACAAGGT-3' Rev: 5'-CAGTATCACCCTTGGCACCAT-3' Probe: 5'-TCCTGCTGGTCCCCGAGGAAACA-3'
<i>Cpt1a</i> NM_013495.1	Fwd: 5'-CTCAGTGGGAGCGACTCTTCA-3' Rev: 5'-GGCCTCTGTGGTACACGACAA-3' Probe: 5'-CCTGGGGAGGAGACAGACACCATCCAAC-3'
<i>Mlxip/Chrebp</i> NM_021455.3/NM_133552.1	Fwd: 5'-GATGGTGCAGAACAGCTCTTCT-3' Rev: 5'-CTGGGCTGTGTCATGGTGAA-3' Probe: 5'-CCAGGCTCCTCCTCGGAGCCC-3'
<i>Cyp26a1</i> NM_007811.1	Fwd: 5'-GGAGACCCTGCGATTGAATC-3' Rev: 5'-GATCTGGTATCCATTCAGCTCAA-3' Probe: 5'-TCTTCAGAGCAACCCGAAACCTCC-3'
<i>Dgat1</i> NM_010046.2/NM_053437.1	Fwd: 5'-GGTGCCCTGACAGAGCAGAT-3' Rev: 5'-CAGTAAGGCCACAGCTGCTG-3' Probe: 5'-CTGCTGCTACATGTGGTTAACCTGGCCA-3'
<i>Dgat2</i> NM_026384.2/NM_001012345.1	Fwd: 5'-GGGTCCAGAAGAAGTCCAGAAG-3' Rev: 5'-CCCAGGTGTCAGAGGAGAAG-3' Probe: 5'-CCCCTGCATCTTCCATGGCCG-3'
<i>Fasn</i> NM_007988/NM_017332	Fwd: 5'-GGCATCATTGGGCACTCCTT-3' Rev: 5'-GCTGCAAGCACAGCCTCTCT-3' Probe: 5'-CCATCTGCATAGCCACAGGCAACCTC-3'
<i>Fgf21</i> NM_020013.4/NM_130752.1	Fwd: 5'-CCGCAGTCCAGAAAGTCTCC-3' Rev: 5'-TGACACCCAGGATTTGAATGAC-3' Probe: 5'-CCTGGCTTCAAGGCTTTGAGCTCC A-3'
<i>Hsd17b13</i> NM_198030.2/NM_001163486.1	Fwd: 5'-AAAGCAGAAAAGCAGACTGGTTCT-3' Rev: 5'-CCCAGTTTCTGCATTTGT-3' Probe: 5'-CGGTTTCTCAACACCAGCTTATTGA-3'
<i>Lipe/HSL</i> NM_010719/X51415	Fwd: 5'-GAGGCCTTTGAGATGCCACT-3' Rev: 5'-AGATGAGCCTGGCTAGCACAG-3' Probe: 5'-CCATCTCACCTCCCTTGGCACACAC-3'
<i>IL-1β</i> NM_008361	Fwd: 5'-ACCCTGCAGCTGGAGAGTGT-3' Rev: 5'-TTGACTTCTATCTTGTGAAGACAAACC-3' Probe: 5'-CCCAAGCAATACCCAAAGAAGAAGATGGAA -3'
<i>IL-6</i> NM_031168	Fwd: 5'-CCGGAGAGGAGACTTCACAGA-3' Rev: 5'-AGAATTGCCATTGCACAACCTT-3' Probe: 5'-ACCACTCACAAGTCGGAGGCTTAATTACA-3'
<i>iNos/Nos2</i> AF049656/NM_010927/NM_012611	Fwd: 5'-CTATCTCCATTCTACTACTACCAGATCGA-3' Rev: 5'-CCTGGCCTCAGCTTCTCAT-3' Probe: 5'-CCCTGGAAGACCCACATCTGGCAG-3'

Supplementary Table 2. Continued

Gene/ID	TaqMan primers and probe
<i>Ldlr</i> NM_010700/NM_175762	Fwd: 5'-GCATCAGCTTGGACAAGGTGT-3' Rev: 5'-GGGAACAGCCACCATTGTTG-3' Probe: 5'-CACTCCTTGATGGGCTCATCCGACC-3'
<i>Lpl</i> NM_008509/NM_012598	Fwd: 5'-AAGGTCAGAGCCAAGAGAAGCA-3' Rev: 5'-CCAGAAAAGTGAATCTTGACTTGGT-3' Probe: 5'-CCTGAAGACTCGCTCTCAGATGCCCTACA-3'
<i>Lrat</i> NM_023624	Fwd: 5'-TCCATACAGCCTACTGTGGAACA-3' Rev: 5'-CTTACGGTGTTCATAGAACCTTCTCA-3' Probe: 5'-ACTGCAGATATGGCTCTCGGATCAGTCC-3'
<i>LRAT</i> NM_004744	Fwd: 5'-TGCGAGCACTTCGTGACCTA-3' Rev: 5'-TTATCTTACAGTCTCACAAAACCTTGTG-3' Probe: 5'-TGCAGATATGGCACCCCGATCAGTC-3'
<i>Pck1</i> NM_011044/NM_198780	Fwd: 5'-GTGTCATCCGCAAGCTGAAG-3' Rev: 5'-CTTTGATCCTGGCCACATC-3' Probe: 5'-CAACTGTTGGCTGGCTCTCACTGACCC-3'
<i>Ppargc1</i> α / <i>Pgc1</i> α NM_008904/NM_031347	Fwd: 5'-GACCCCAGAGTCACCAAATGA-3' Rev: 5'-GGCCTGCAGTTCAGAGAGT-3' Probe: 5'-CCCCATTTGAGAACAAGACTATTGAGCGAACCC-3'
<i>Pnpla2/Atgl</i> NM_025802/XM_347183	Fwd: 5'-AGCATCTGCCAGTATCTGGTGAT-3' Rev: 5'-CACCTGCTCAGACAGTCTGGAA-3' Probe: 5'-ATGGTCACCCAATTTCTCTTGGCCC-3'
<i>Pnpla3</i> NM_054088	Fwd: 5'-ATCATGCTGCCCTGCAGTCT-3' Rev: 5'-GCCACTGGATATCATCCTGGAT-3' Probe: 5'-CACCAGCCTGTGGACTGCAGCG-3'
<i>PNPLA3</i> NM_025225	Fwd: 5'-CTGTACCCTGCCTGTGGAATCT-3' Rev: 5'-AGGACATCGTCGGGCATATCT-3' Probe: 5'-CCATGTCACCAGTCTCTGGACAATCGC-3'
<i>RAR-β</i>	Assay on demand, Mm01319677_m1 (ThermoFisher)
<i>Raldh1</i>	Assay on demand, Mm00657317_m1 (ThermoFisher)
<i>Raldh2</i>	Assay on demand, Mm00501306_m1 (ThermoFisher)
<i>Raldh3</i>	Assay on demand, Mm00474049_m1 (ThermoFisher)
<i>Raldh4</i> NM_178713.4	Fwd: 5'-TGGAGCAGTCTCTGGAGGAGTT-3' Rev: 5'-GAAGTTCAGAACAGACCCGAGGAA-3' Probe: 5'-AATCTAAAGACCAAGGGAAAACCTCACGC-3'
<i>Rbp4</i> NM_011255.2/XM_215285.3	Fwd: 5'-GGTGGGCACTTTCACAGACA-3' Rev: 5'-GATCCAGTGGTCATCGTTTCCT-3' Probe: 5'-CCCCAGTACTTCATCTTGAACCTGGCAGG-3'
<i>Scd1</i> NM_009127.2	Fwd: 5'-ATGCTCCAAGAGATCTCCAGTTCT-3' Rev: 5'-CTTACCTTCTCTCGTTTCATTCC-3' Probe: 5'-CCACCACCACCATCACTGCACCTC-3'
<i>TGF-β1</i> NM_021578.1	Fwd: 5'-GGGCTACCATGCCAACTTCTG-3' Rev: 5'-GAGGGCAAGGACCTTGCTGTA-3' Probe: 5'-CCTGCCCTACATTTGGAGCCTGGA-3'
<i>TGF-β1</i> NM_021578.1	Fwd: 5'-GGGCTACCATGCCAACTTCTG-3' Rev: 5'-GAGGGCAAGGACCTTGCTGTA-3' Probe: 5'-CCTGCCCTACATTTGGAGCCTGGA-3'
<i>Timp1</i> NM_001044384.1/NM_011593.2	Fwd: 5'-TCTGAGCCCTGCTCAGCAA-3' Rev: 5'-AACAGGGAAACACTGTGCACAC-3' Probe: 5'-CCACAGCCAGCACTATAGGTCTTTGAGAAAGC-3'
<i>TNF-α</i> NM_013693/NM_012675	Fwd: 5'-GTAGCCACGTCGTAGCAAAC-3' Rev: 5'-AGTTGGTTGTCTTTGAGATCCATG-3' Probe: 5'-CGCTGGCTCAGCCACTCCAGC-3'
<i>Ucp2</i> NM_011671.2	Fwd: 5'-CGAAGCCTACAAGACCATTGC-3' Rev: 5'-ACCAGCTCAGCACAGTTGACA-3' Probe: 5'-CAGAGGCCCCGGATCCCTTCC-3'